AD-A045 053 CALSPAN CORP BUFFALO N Y F/G 4/2
THREE-DIMENSIONAL STRUCTURE OF CONVECTIVE STORMS AND THE ROLE O--ETC(U)
SEP 77 C W ROGERS N00014-75-C-0979
UNCLASSIFIED CALSPAN-CK-5976-M-1 NL

| OF |
AD
A045 053

END
DATE
FILMED
11-77
DDC

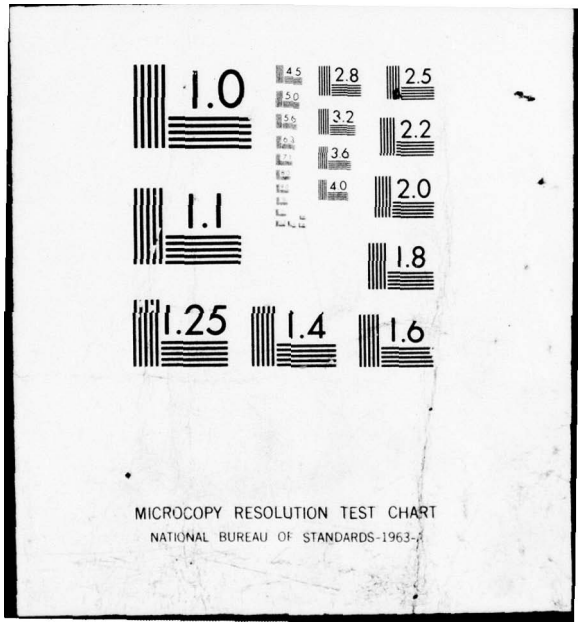
1.0
1.1
1.25
1.4
1.6
1.8
2.0
2.2
2.5
2.8
3.2
3.6
4.0
4.5
5.0
5.6
MICROCOPY RESOLUTION TEST CHART
NATIONAL BUREAU OF STANDARDS-1963-A

(12)

Calspan

Technical Report

Calspan Corporation
Buffalo, New York 14221

Calspan

THREE-DIMENSIONAL STRUCTURE OF CONVECTIVE STORMS AND THE ROLE OF VERTICAL SHEAR IN STORM LIFE CYCLE

C. William Rogers

Calspan Report No. CK-5976-M-1

Prepared For:
METEOROLOGY DIVISION
NAVAL AIR SYSTEMS COMMAND
DEPARTMENT OF THE NAVY
WASHINGTON, D. C. 20361

SEPTEMBER 1977
CONTRACT NO. N00014-75-C-0979
FINAL REPORT

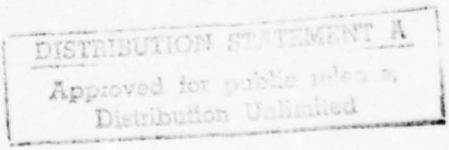

Calspan Corporation
Buffalo, New York 14221

Unclassified

SECURITY CLASSIFICATION OF THIS PAGE (When Data Entered)

REPORT DOCUMENTATION PAGE	READ INSTRUCTIONS BEFORE COMPLETING FORM
1. REPORT NUMBER: CALSPAN-CK-5976-M-1	2. GOVT ACCESSION NO. / 3. RECIPIENT'S CATALOG NUMBER
4. TITLE (and Subtitle): Three-dimensional Structure of Convective Storms and the Role of Vertical Shear in Storm Life Cycle,	5. TYPE OF REPORT & PERIOD COVERED: Final Report. 1 Apr 75 - 30 Sep 76; 4/1/75 - 9/30/76
	6. PERFORMING ORG. REPORT NUMBER
7. AUTHOR(s): C. William Rogers	8. CONTRACT OR GRANT NUMBER(s): N00014-75-C-0979
9. PERFORMING ORGANIZATION NAME AND ADDRESS: Calspan Corporation, Buffalo, New York 14221	10. PROGRAM ELEMENT, PROJECT, TASK AREA & WORK UNIT NUMBERS
11. CONTROLLING OFFICE NAME AND ADDRESS: Office of Naval Research, Department of the Navy, Arlington, Virginia 22217	12. REPORT DATE: September 1977
	13. NUMBER OF PAGES: 52 (12 56p.)
14. MONITORING AGENCY NAME & ADDRESS (if different from Controlling Office): Meteorology Division, Naval Air Systems Command, WAshington, D.C. 20361	15. SECURITY CLASS. (of this report): Unclassified
	15a. DECLASSIFICATION/DOWNGRADING SCHEDULE

16. DISTRIBUTION STATEMENT (of this Report)

Distribution unlimited.

DDC RECEIVED OCT 11 1977 C

17. DISTRIBUTION STATEMENT (of the abstract entered in Block 20, if different from Report)

18. SUPPLEMENTARY NOTES

19. KEY WORDS (Continue on reverse side if necessary and identify by block number)

Convective Storm Life Cycle
Three-Dimensional Structure
Vertical Wind Shear
Doppler Radar

20. ABSTRACT (Continue on reverse side if necessary and identify by block number)

A model is presented which describes the three-dimensional location of the updraft in a convective storm as a function of the wind velocity in the low-level inflow to the storm and the storm's motion. This updraft-plane model was used to interpret doppler velocities in RHI scans. It was found that (1) the plane containing the updraft is oriented at an angle to the direction of storm motion; (2) the convective storm as defined by its radar echo is not just an upward sloping updraft overlying a downward sloping

7 over

DD FORM 1 JAN 73 1473 EDITION OF 1 NOV 65 IS OBSOLETE

Unclassified

SECURITY CLASSIFICATION OF THIS PAGE (When Data Entered)

407727

20.

downdraft but it also contains environmental air which flows horizontally under the updraft, receives precipitation from it, and transports the precipitation downwind. Application of this precipitation transport concept to severe right moving storms suggests that the turn of the storm track to the right of the mean wind direction occurs in the storm's life cycle when precipitation falls into mid-levels whose wind direction is strongly veered to the right of the mean wind.

cont. → The updraft-plane model led to the following hypothesis on the role of vertical shear in the environmental wind in controlling the life cycle of convective storms. If there is an alignment between the horizontal velocity of the middle level air in which the downdraft originates and the orientation and motion of the updraft plane, then the downdraft air, as it sinks through the storm toward the ground, will continually find itself underneath the updraft such that precipitation evaporation and precipitation loading may maintain and strengthen the downdraft. Conversely, if an alignment is not present, then the downdraft may not be maintained and the convective storm may be of the short-lived type.

Acknowledgements

Roland Pilié deserves special thanks for his help during the project, and in particular for his advice concerning the makeup of this report. I am deeply indebted to Gene Mack for his painstaking review of the report and for his many helpful suggestions during its preparation. George Zigrossi was invaluable to this project both for his maintenance of the doppler radar and for the many long hours spent in the field during data acquisition. We acknowledge the cooperation and aid furnished by the U.S. Forest Service during the three field years in Georgia. Finally, I wish to express my gratitude to Calvin Easterbrook for the opportunity to participate in this project and for the long and fruitful relationship which we shared.

Table of Contents

List of Figures

List of Figures (Cont.)

Section 1
INTRODUCTION

In recent years application of doppler radar to convective storms has provided increasing insight into the internal flow patterns of these systems. Tornado producing storms have been studied in the National Severe Storms Laboratory area in Oklahoma and hail producing storms have been studied in the National Hail Research Experiment region in Colorado. In 1972 under sponsorship of the Naval Air Systems Command, Calspan Corporation began a study of the airflow within convective storms occurring in the vicinity of a U. S. Navy-Forest Service surface meso-network located in coastal Georgia. Doppler velocities were measured within the convective storms by the Calspan doppler radar while surface weather observations were acquired by the mesonetwork stations maintained and operated by the U. S. Forest Service. Radiosonde data and WSR-57 radar observations were taken at nearby Waycross, Ga.

During the first two years of this program, research was directed toward refining a method to obtain the horizontal wind field at very low levels in convective storms by applying two-dimensional curve fitting techniques to doppler velocity fields. This work was reported on fully in three previous contract reports (Easterbrook and Rogers, 1973, 1974 and Easterbrook, 1974) and in a paper presented at the 16th Radar Meteorology Conference (Easterbrook, 1975). During the final two years, attention was shifted to obtaining information about the three-dimensional air flow in convective storms by interpretation of RHI scans of doppler velocity. In the final year no field program was carried out but data reduction was performed on previously observed but unanalyzed convective storms. Much of the latter contract effort was directed toward interpretation of the structure of the convective storms studied during the program.

The primary result of this study was a model which describes the three-dimensional location of the updraft in a convective storm as a function of the wind velocity in the low-level inflow to the storm and the storm's motion. This updraft-plane model facilitates examination of the interaction between the environmental air and the updraft, principally as a function of height. Since vertical shear enters into the variation of this interaction

with height, the model can be and was utilized to examine the influence of vertical shear on the behaviour and life cycle of convective storms.

Section 2 of this report presents a summary of results concerning the role of vertical shear in the behaviour and life cycle of convective storms and recommendations for further study. Section 3 presents 1.) a description of the updraft-plane model; 2.) application of the model to motion of the radar echo associated with convective storms, in particular severe right moving storms; and 3.) application of the model to maintenance of downdrafts in convective storms. Section 4 presents a detailed discussion of the convective storms analyzed during the final year of the program.

Section 2
SUMMARY OF RESULTS AND RECOMMENDATIONS

2.1 Results

The primary results of this study were obtained by using the updraft-plane model to interpret observations of convective storms. The model was applied both to convective storms studied by Calspan at the Georgia field site and to storms studied by other groups at various field sites. The results cover convective storm structure, radar echo motion, and maintenance of downdrafts.

Before proceeding to a presentation of convective storm structure it is necessary to define what is meant by an updraft in this discussion. Throughout the vertical extent of a convective storm there are rising parcels of air. At any instant of time, a line drawn through and connecting the center of these parcels, starting near the ground and extending to the top of the storm, is called the updraft. This line is not to be thought of as a streamline or a trajectory, but only the locus of parcels which are rising. A similar definition applies to the downdraft, which originates in middle levels and extends to the ground.

2.1.1 Convective Storm Structure

The following conclusions concerning storm structure were derived from the cases studied in the Calspan-Georgia program.

(1) Rising parcels which originate in low-level environmental air produce an updraft which slopes upward away from the direction of storm movement and which is located at an angle counterclockwise from the direction of storm motion.

(2) The downdraft originates in dry, mid-level environmental air which enters the storm directly underneath the updraft at the rear of the storm. The downdraft extends downward to the earth's surface in the direction of storm motion.

(3) *Between the ground and the mid level of the storm,* regions of precipitation which exist outside both the updraft and downdraft contain environmental air moving only horizontally. Near the updraft the environmental air is deflected as it flows around the updraft. Away from the updraft the air moves with its environmental direction. Thus lower level environmental air which is moving only horizontally is located near the centroid of the radar echo as well as in the periphery.

This storm structure is similar to previously determined storm structures with respect to the location of source regions of the updraft and downdraft and to the slope of the updraft and downdraft within the storm. However, this storm structure differs from previously observed storm structures in that 1.) the plane containing the updraft is oriented at an angle to the direction of storm motion; and 2.) the environmental flow participates in the radar echo not only in the updraft and downdraft but as horizontally moving air in other parts of the storm.

The convective storm as defined by its radar echo thus is not just an obstacle around which the environmental air flows. Rather the radar echo contains an upward sloping updraft under and around which environmental air moves while receiving precipitation from the updraft above. Of this environmental air, that which possesses the necessary dryness for downdraft formation becomes the source of the downdraft. That environmental air which is too moist for downdraft formation transports the precipitation downwind. With this picture of environmental air's participation in convective storms, an examination of the interaction with height between a sloping updraft and the environmental flow in which it is imbedded can provide insight into how vertical shear in the environmental wind influences the behaviour and life cycle of convective storms.

2.1.2 Radar Echo Motion

The participation of environmental air in the radar echo suggests that radar echo motion represents an ensemble motion of precipitation: i.e. that carried by horizontally moving environmental air, and generation and

dissipation and horizontal movement of precipitation contained in the updraft and downdraft. Application of this ensemble concept to severe right moving storms suggests that the turn of the storm track to the right of the mean wind direction occurs in the storm's life cycle when precipitation falls into mid levels whose wind direction is strongly veered to the right of the mean wind. Since precipitation fallout does not reach a maximum until after the initial storm stage, at the time the updraft grows to heights above mid levels, a turn of the storm to the right of the mean wind should not be observed until after a storm reaches this stage.

2.1.3 Downdraft Maintenance

Application of the updraft-plane model to the question of the generation of downdrafts led to a hypothesis of the role of vertical shear in the environmental wind in controlling the life cycle of convective storms. If the updraft in a convective storm is triggered by forced lifting above the downdraft near the surface and if the downdraft is maintained by precipitation evaporation and precipitation loading underneath the updraft, then the updraft-downdraft couplet forms an interdependent system.

This hypothesis postulates an alignment between the horizontal velocity of the middle level air in which the downdraft originates and the orientation and motion of the updraft plane. If this alignment exists then the downdraft, as it sinks through the storm toward the ground, will continually find itself underneath the updraft and continuously in position to receive precipitation. This configuration between updraft and downdraft might be optimum for the maintenance of the updraft-downdraft couplet and appears to be a configuration which promotes long-lived storms such as the severe, right moving variety. Conversely, if the alignment is not satisfied, then the convective storms may be of the short-lived type. By testing this hypothesis some insight may be gained into the influence of vertical shear in the environmental wind on the behaviour and life cycle of convective storms.

2.2 Recommendations

A first step in future study of the possible alighment relationship between updraft and downdraft should involve numerical modeling. The updraft features and the distribution of precipitation in the vertical could come from current one-dimensional numerical models. The vertical distributions of precipitation and updraft speed would be located horizontally by the updraft plane motion and orientation. The evolution of conditions in the downdraft parcel could then be obtained by a Lagrangian integration in which the precipitation experienced by the downdraft parcel would be supplied from the updraft integration and the updraft plane model. Such a study would allow examination of the variation in downdraft evolution as a function of vertical shear in the environmental wind, both by varying the horizontal velocity of the downdraft source parcel and the orientation of the updraft plane. This approach would have the added, decided advantage of producing a quasi-three dimensional simulation of the downdraft without having to perform time dependent integrations in three dimensions.

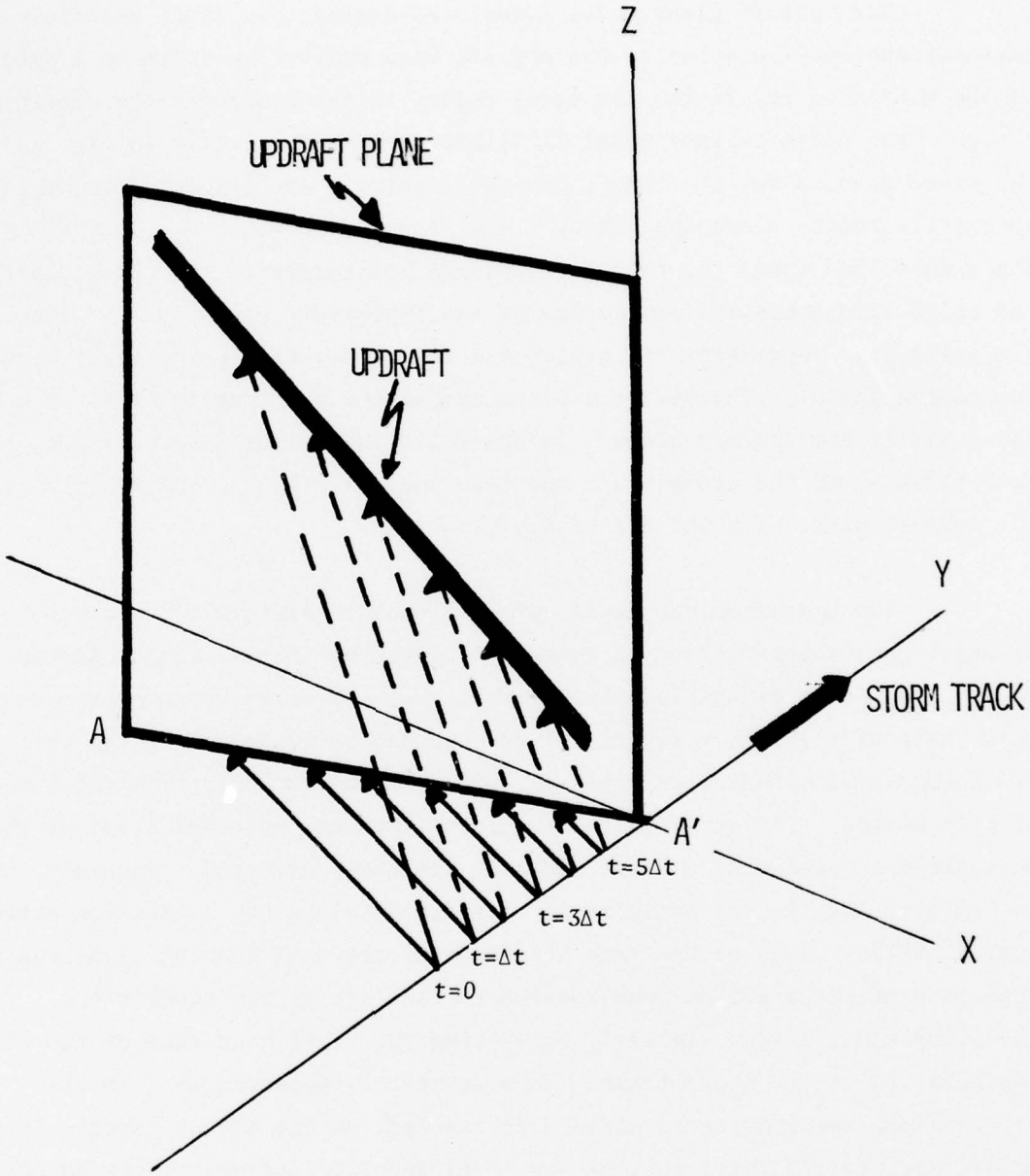

Figure 1 Schematic of updraft plane, three-dimensional trajectories of updraft source parcels (dashed lines) and storm track.

Section 3
UPDRAFT-PLANE MODEL

The updraft-plane model formulated during this study describes the three-dimensional location of the updraft in a convective storm as a function of the wind velocity in the low-level inflow to the storm and the storm's motion. The updraft-plane model is illustrated schematically in Fig. 1. As the storm moves along its track, low-level parcels are triggered to rise at successive points along the track, $t = 0$, $t = \Delta t$, $t = 2\ \Delta t \ldots$, $t = 5\ \Delta t$. The dashed line shows the three-dimensional trajectory of the parcel while the solid line shows the projection of the trajectory onto the X-Y plane. The solid line represents the horizontal motion due to the low-level wind of the source parcel. The vertical plane containing the updraft at $t = 6\ \Delta t$ is shown and is the updraft plane. In the following discussion we will be concentrating on the storm track and the line given by the intersection of the updraft plane with the X-Y plane, line A-A'.

The updraft-plane model was developed to explain two characteristics of radar echoes observed on 23 June 1974 by the WSR-57 located at Waycross, Ga. (For detailed discussion, see Section 4.) First it was observed that the major axis of the high reflectivity core was not oriented along the cell track but was located at an angle of $> 90°$ counterclockwise from the direction of cell motion. This observation suggested that the vertical plane of the precipitation producing updraft might be similarly oriented. Secondly, it was noticed that in the early stage of storm development, a line connecting successive positions of the left hand edge of the echo(looking along the direction of storm motion) was rotated to the left of the storm track. On the other hand, a line similarly connecting the right hand edge of the echo was parallel to the storm track. This structure suggested that in its early stages the radar echo widened to the left as the rising parcels in the updraft maintained their initial low-level velocity and new rising parcels formed on the right edge of the echo along a line parallel to the echo track.

The updraft-plane model provides the orientation of the vertical plane of the updraft relative to the storm track using as input only the storm velocity and low-level wind velocity. The model assumes that:

(1) the updraft begins in air flowing near the earth's surface;

(2) the updraft air conserves its horizontal velocity as it rises;

(3) the low-level parcels which originate the updraft are triggered at successive points along a line oriented parallel to the direction of motion of the radar echo.

The orientation of the updraft plane is obtained by a graphical construction in which the spacing between successive low-level source-parcels is scaled by the speed of the radar echo. In addition the scaling determines the horizontal displacement of each rising parcel during the time interval which elapses between the triggering of successive source parcels. Consider as an example the following graphical construction of an updraft plane.

3.1 Example of Updraft-Plane Graphical Construction

An updraft plane constructed from this model is shown in Fig. 2. The inputs to the construction were a horizontal echo velocity of 15m/sec from 257° and a low-level air velocity of 12m/sec from 243° (data for Cell C, 23 June 1974, discussed in Section 4 .) The line A-A' is the horizontal projection of the locus of rising parcels at an arbitrary time and defines the location of the vertical plane containing the updraft. The base of the updraft is located at A' and the higher levels are at A. The successive source-location for low-level parcels along the track are labeled as $t = 0$, $t = \Delta t$, etc. The source parcel triggered at $t = 0$ travels to B by $t = 4 \Delta t$. Source parcels triggered earlier than $t = 0$ are located along AB; those triggered later are located along BA'.

3.2 Application of the Updraft-Plane Model to Interaction between the Updraft and Environmental Winds

The updraft-plane model provides a framework for investigating

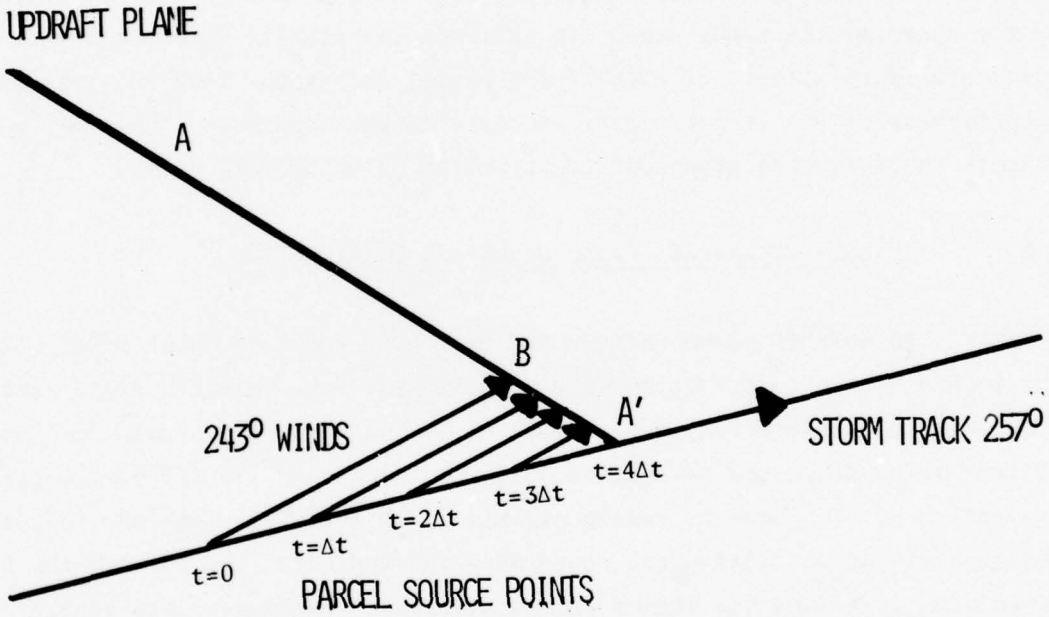

Figure 2 Example of graphical construction of updraft plane.

the interaction between the updraft and the environmental winds. Fig. 3 is a three-dimensional schematic illustrating the use of the model. A horizontal plane is located at mid-level, labeled (1). The environmental wind for level (1) is shown in a location such that it does not encounter the updraft at level (1), and flows under the updraft located at the higher level (2). As the air flows under the updraft it receives precipitation from level (2) and distributes it into the region of the radar echo outlined on the plane at level (1). This process of horizontal distribution of precipitation by undisturbed environmental air is the major feature of the following applications of the updraft model. However, again the discussion will use the projection of the updraft plane onto the X-Y plane, and the winds in the convective layer will be labeled by the height at which they occur.

Fig. 4 shows two consecutive, constructed updraft planes (at $t = 0$ and $t = \Delta t$) separated by a displacement given by the cell speed, and shows appropriately scaled displacements for the environmental air located underneath the updraft at $t = 0$. If it is assumed that the rising parcels in the updraft maintain their horizontal velocity as they rise, then the vertical shear determines how the environmental air at various levels moves with respect to the updraft plane. The height of the updraft is indicated along the updraft plane at $t = 0$. Selected wind vectors from the appropriate Waycross radiosonde (1800GMT 23 June 1974) are depicted by the arrows on the figure. The arrows thus show the horizontal motion of the environmental air. Comparison of the endpoints of the arrows and the updraft plane at $t = \Delta t$ shows the motion of the environmental air relative to the updraft plane in time Δt. In the 1.5 to 3.5km layer and again around 7 km the air overtakes the updraft plane, while in the layer between 4 and 6km, the environmental air lags behind the updraft plane.

3.2.1 Radar Echo Motion and Environmental Winds

The relative position between environmental air and the updraft as depicted in Fig. 4 can be used to examine how precipitation is distributed after it falls from the updraft. For the purposes of illustration assume that precipitation falls from the updraft along the height interval 2-7km in Fig. 3. The precipitation is then distributed horizontally by the environmental winds

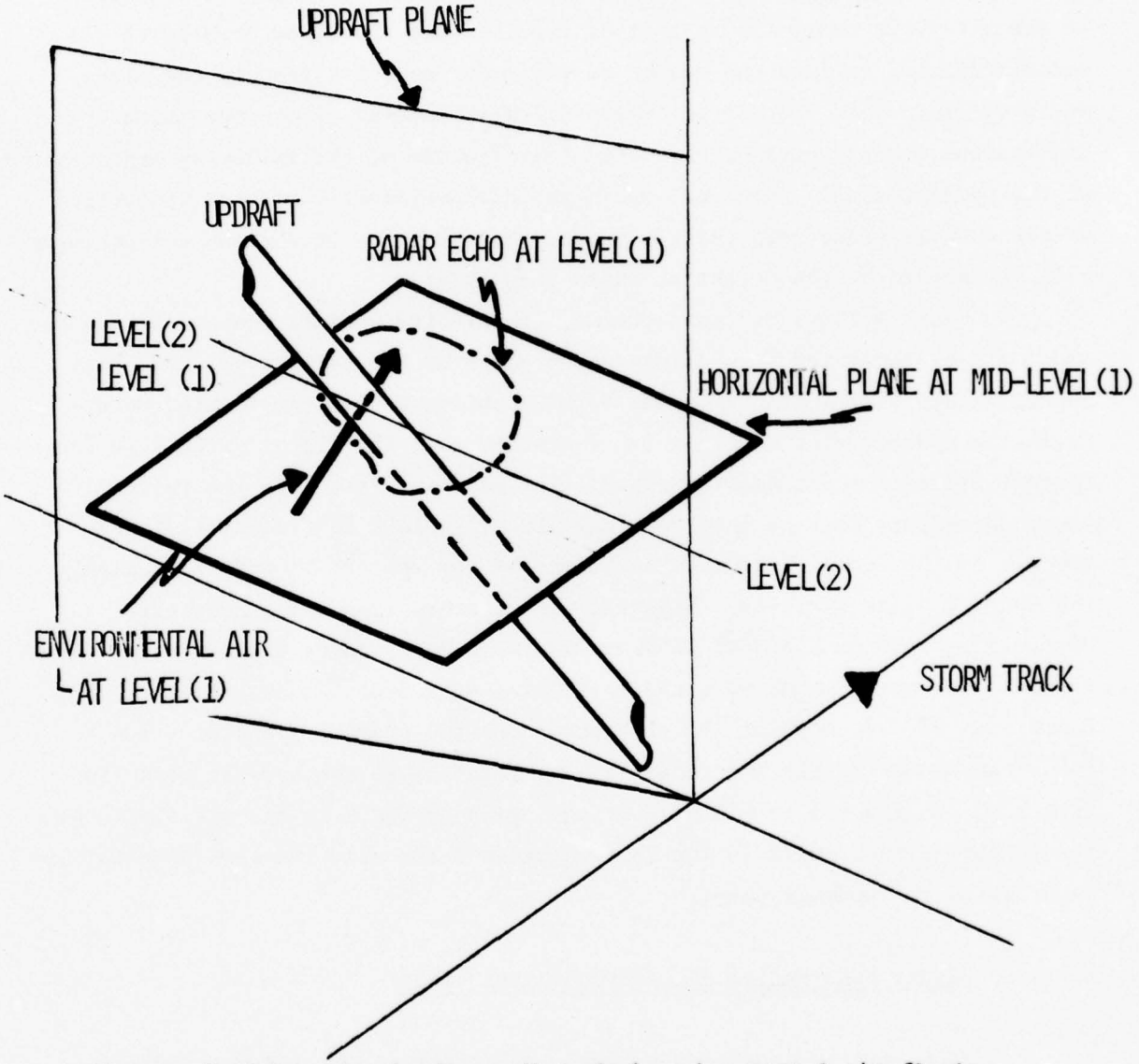

Figure 3 Schematic showing undisturbed environmental air flowing underneath a sloping updraft.

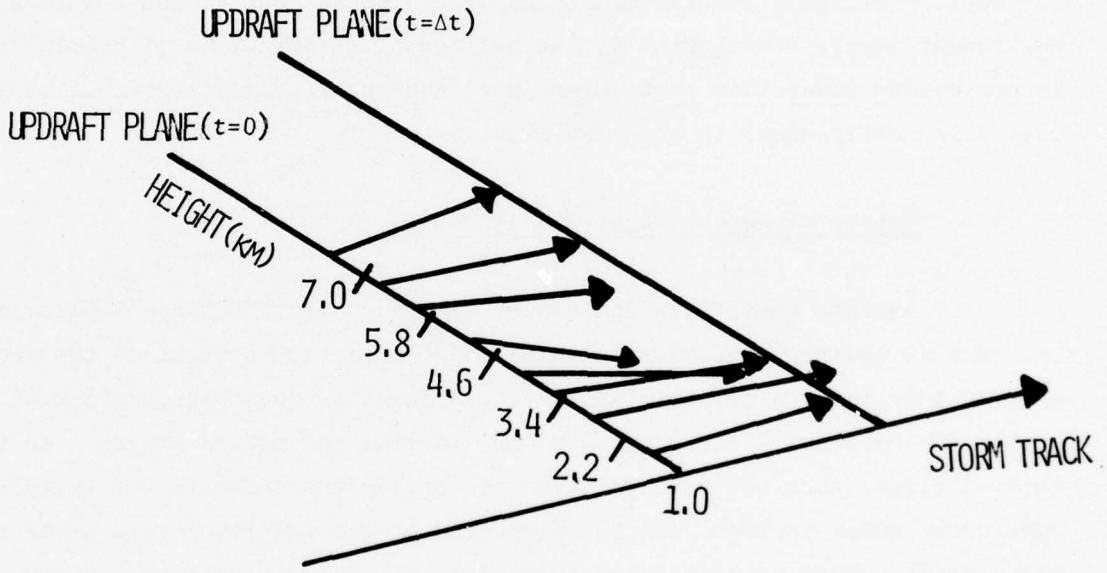

Figure 4 Relative horizontal motion between updraft plane and environmental air, June 23, 1974.

through which it falls. Thus the radar echo consists of the sum of the precipitation contained in the updraft and downdraft and that which is distributed horizontally by the environmental wind field.

Viewing the radar echo in this light provides some insight into the motion of echo centroids as a function of the vertical shear in the environmental air. For example, the winds shown in Fig. 4 veer with height up to 5.5km and then back above that level to an altitude of 7.6km (winds were not measured above 7.6km) producing a mean wind of 15m/sec at 261°. The velocity of the radar echo, based on echo centroid movement, was 15m/sec at 257°. Because of the relatively uniform wind speed (15m/sec) and both the veering and backing of the wind direction, the mean wind was not biased toward any particular layer. Consequently, the horizontal distribution of precipitation is not biased toward any particular layer and the resultant ensemble cell motion is nearly equal to the mean wind.

3.2.2 Motion of Severe Right Moving Storms

Another question which can be examined with the updraft-plane model is: Why do severe right moving storms (SRM) turn to the right of the mean wind as they reach a steady state? To examine this question consider the motion of the storm's radar echo in the initial and mature stages. In the initial stage, when the precipitation is largely suspended in the updraft, the radar echo moves primarily in the direction of the low-level wind present in the updraft. When precipitation falls from the updraft into the environmental air beneath the updraft, horizontal distribution of precipitation by the environmental wind becomes important in producing the motion of the radar echo. SRM storms occur under conditions of strong directional and speed shear in which winds in the middle and upper levels are stronger and veered relative to the low-level winds present in the updraft. Since the strong updrafts in these storms extend to great heights, fallout of precipitation occurs initially into middle and upper levels. The horizontal distribution of precipitation is then biased toward the wind velocity at the mid to upper levels, and the echo centroid moves to the right of the mean wind in the

convective layer.

As an example of a SRM storm consider one studied by Fankhauser (1971). The updraft plane for the SRM stage of this storm, selected environmental winds, and the mean wind of 231° at 17m/sec are shown in Fig. 5. In the severe right moving state, precipitation was carried to the right of the mean wind, e.g. by the 500 mb wind of 258° at 16m/sec, and the radar echo moved to the right of the mean wind at 259° at 9m/sec. Thus in the SRM stage the storm showed a track to the right of the mean wind as precipitation was carried by the upper level environmental winds ahead and to the right of the mean wind.

3.2.3 Differentiation of Horizontally Moving Air from the Updraft in the Radar Echo

The central feature of the two previous discussions was that at all levels there was an angle in the horizontal between the sloping updraft and the environmental wind. As a consequence of this structure it is possible for horizontally moving environmental air, which receives its precipitation from an overlying updraft, to be present near the centroid of the radar echo. Other case studies of convection were also examined to determine if horizontally moving air was present near the echo centroid and if so, what impact such an interpretation might have on those studies.

Brown and Crawford (1972) studied the high reflectivity radar core acting as an obstacle to the environmental flow by comparing simulated flow around a cylinder to observed flow in a convective storm. The observed and simulated flows are shown in Fig. 6. There is good agreement between the two flows except in the east-northeast sector (A), where the observed flow was -25m/sec. and the simulated flow was -10m/sec.

The updraft plane for this storm (construction shown in Fig. 7) was oriented along 205° with the higher levels of the updraft to the north. The updraft plane is entered on Fig. 6a using the 60 dbz contour as the updraft at 6km (B). Drawn from (B) is the wind velocity for the 5.5km level, the level

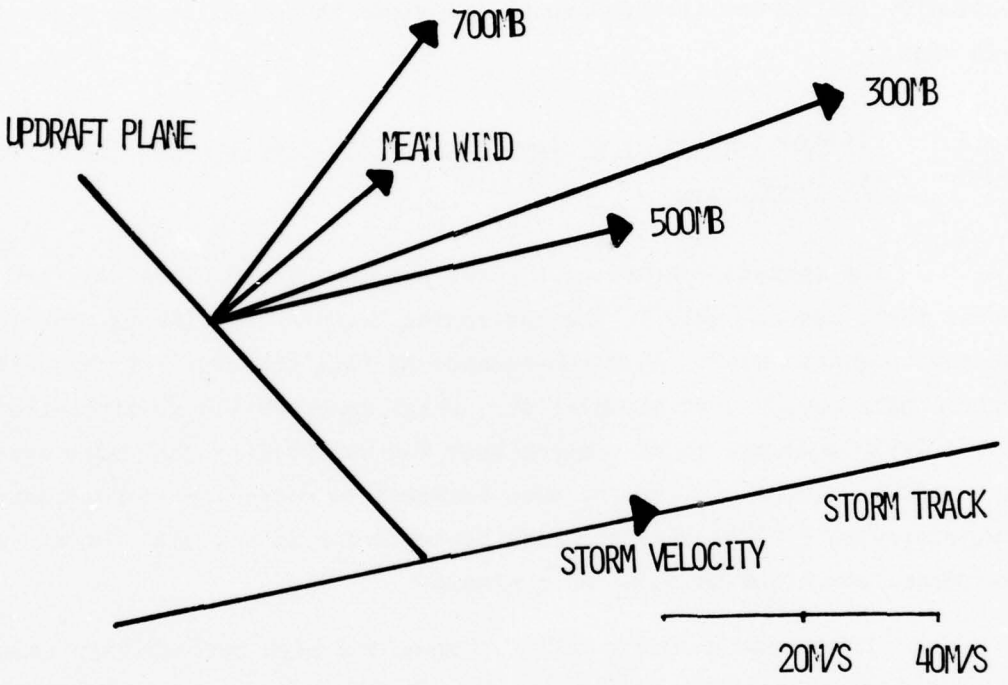

Figure 5 Updraft plane analysis for a severe right moving storm.

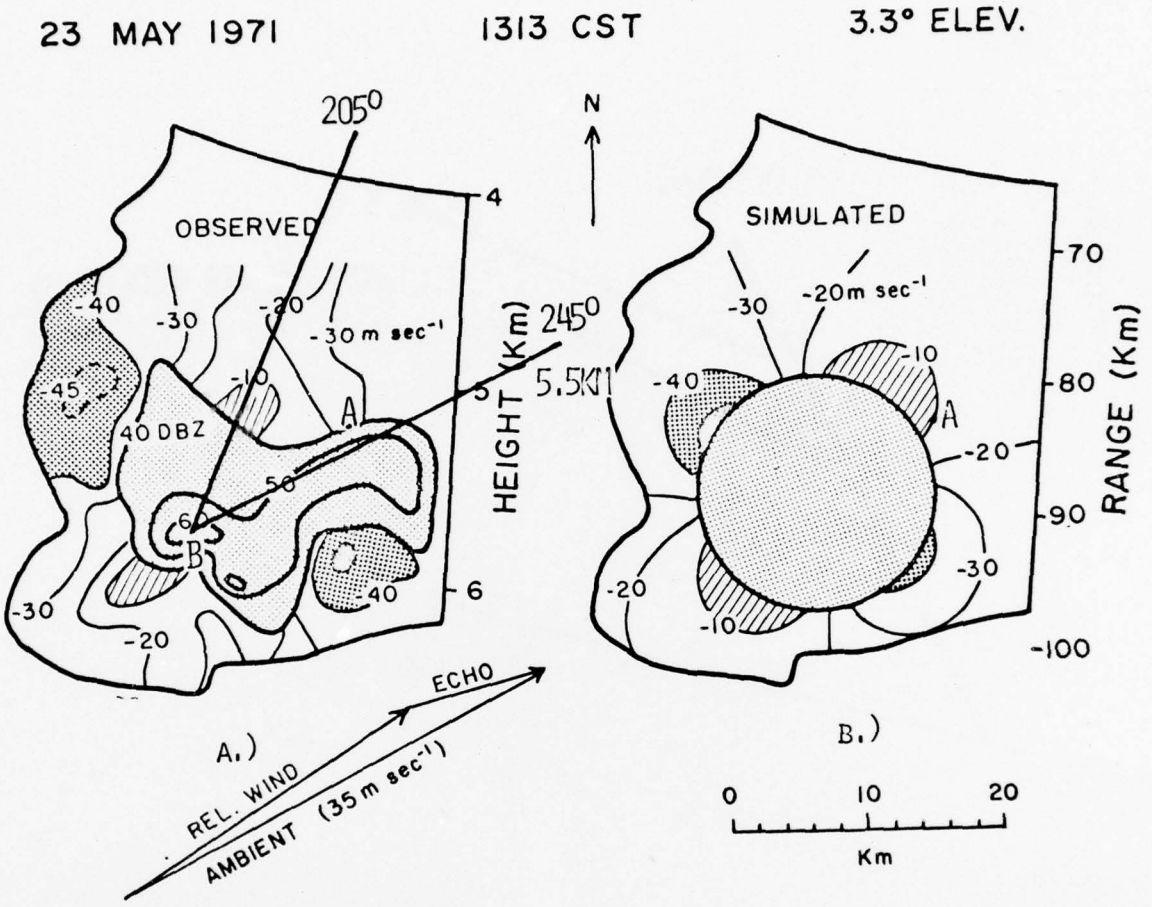

Figure 6 Simulated single Doppler velocity measurements in potential flow around a moving solid cylinder as compared with the Doppler velocities actually measured (i.e., relative to the radar) in the vicinity of the storm's reflectivity core. All velocities in the figure are toward the radar (negative). The heaviest stippled shading represents Doppler velocities in excess of 50 m sec^{-1}. (Brown and Crawford, 1972)
205^{o} updraft plane and 245^{o} wind direction at 5.5km are also shown.

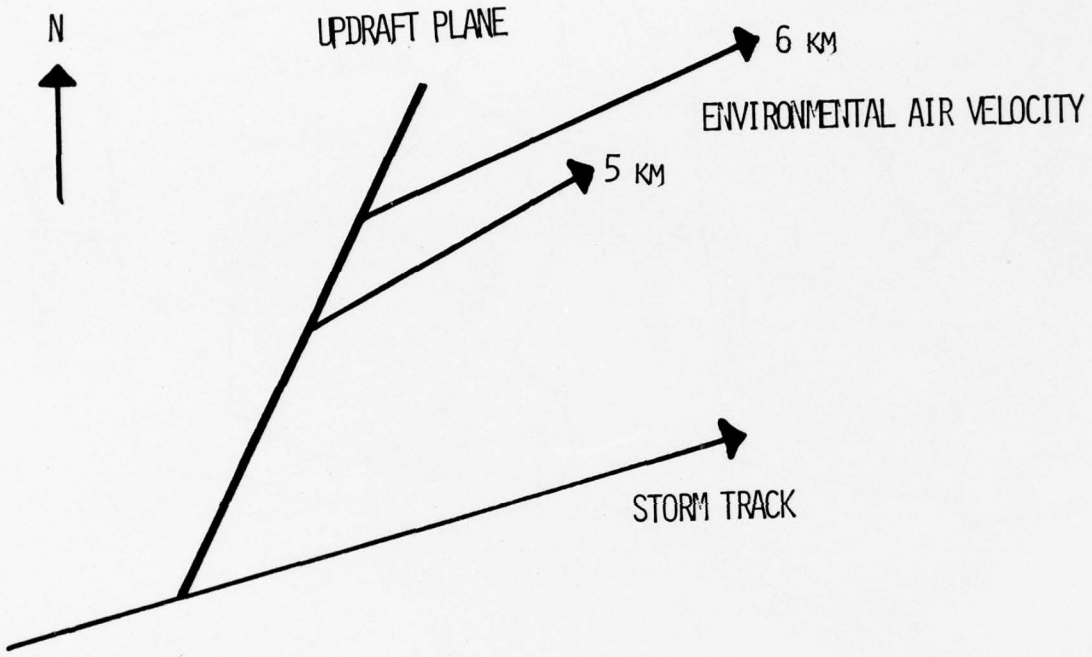

Figure 7 Updraft plane analysis for storm studied by Brown and Crawford (1972, Fig. 6).

which would receive precipitation from the updraft at 6 km. The extension east-northeast from (B) of the area greater than 50dbz parallels the 5.5km wind velocity and indicates that this high reflectivity core at 5.5km was horizontally moving air at that level and not an updraft with flow around it. The -25m/sec observed speed at (A) is environmental flow undisturbed and could not be duplicated by similation of the flow around a cyclinder. Thus the simulated and observed flow are very similar when the region containing the horizontally moving environmental air near point (A) is eliminated from the comparison.

3.3 Possible Role of Vertical Shear in Controlling Downdraft Maintenance

Kropfli and Miller (1975) analyzed the flow within a convective storm using dual doppler measurements. In their discussion they point out "... the gust front on the storm's right forward flank at the surface had its source on the left rear flank at 5.5km." An updraft plane analysis (Fig. 8) applied to this storm indicated that air entering the storm at 5km under the updraft at the left rear would pass through the storm and emerge on the right front. The analysis suggests that while moving through the storm this air would continually find itself underneath the updraft as it sank to the surface. Merging the dual doppler and updraft-plane analyses of this storm suggests that the downdraft which eventually produced the gust front at the surface was driven by precipitation falling into it, probably over a large portion of the air's passage through the storm.

Both the Kropfli and Miller case and the cases studied in this report suggest that an optimum configuration to produce a strond downdraft could exist when a downdraft parcel moves with a velocity such as that as the air moves forward and downward it is always under the updraft. This alignment would help perpetuate the storm by providing a strong downdraft at the surface for triggering the low level parcels which form the roots of the updraft. For example, it could be that the vertical shear in the environmental wind necessary for an inphase configuration between downdraft source air and the

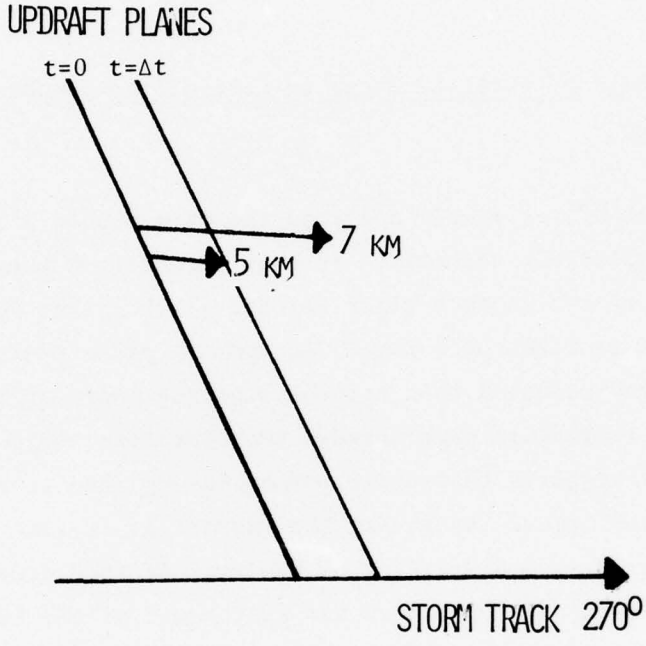

Figure 8 Updraft plane analysis for storm studied by Kropfli and Miller (1974).

updraft is the same as that found to accompany severe right moving storms. If shear is a controlling factor in producing the inphase relationship, then the updraft-plane model provides a framework for research on this question. In addition, if the inphase relationship is found to be valid, then the updraft plane model could be used in forecasting to identify the potential for SRW storms.

Section 4

DISCUSSION OF THE SITUATION OF 23 JUNE 1974

The observed convective storms which lead to the updraft plane concept occurred in southern coastal Georgia during the afternoon and evening of 23 June 1974. A northeast-southwest oriented cold front located in northwestern Ga. at 0800EDT progressed southeastward during the day and was situated along the Ga. coast at 0800EDT on the 24th. At 0800EDT on the 23rd a 500mb trough ran north-south from Ohio to Alabama; this trough was still west of coastal Ga. on the morning of the 24th.

A PPI scan taken by the WSR-57 at Waycross, Ga. (120km west of the Calspan doppler radar) at 1737EDT on the 23rd is shown in Fig. 9. Also shown is the location of the Calspan doppler radar and the circle of maximum unambiguous range (30km) for the doppler radar. The location, time, and shape of cells when the radar echos were first observed are shown on the figure. Cells A, B, and C were sampled by the doppler radar, cell A during the period 1740-1800EDT and cells B and C during the period 1806-1842EDT. These cells moved from 250-260° at approximately 15m/sec.

The Waycross special radiosonde taken at 1400EDT for the Calspan program is shown in Fig. 10. The dew point starts to decrease with altitude at 2.5km and is very low above 5km. A transition zone containing both dry and moist layers exists between 3.5 and 5km; cloud base was at 1.5km.

The wind hodograph for this sounding is shown in Fig. 11. The wind field was characterized by wind speeds of 15 to 18m/sec with a rapid veering of wind direction between 3 and 4km and a corresponding rapid backing between 5.7 and 6.4km.

The doppler radar observations consisted of PPI and RHI scans through the storms for which doppler velocity and signal strength were recorded. The PPI scans were taken at elevation angles below 10°, and because of the small unambiguous range of the radar, all data were obtained

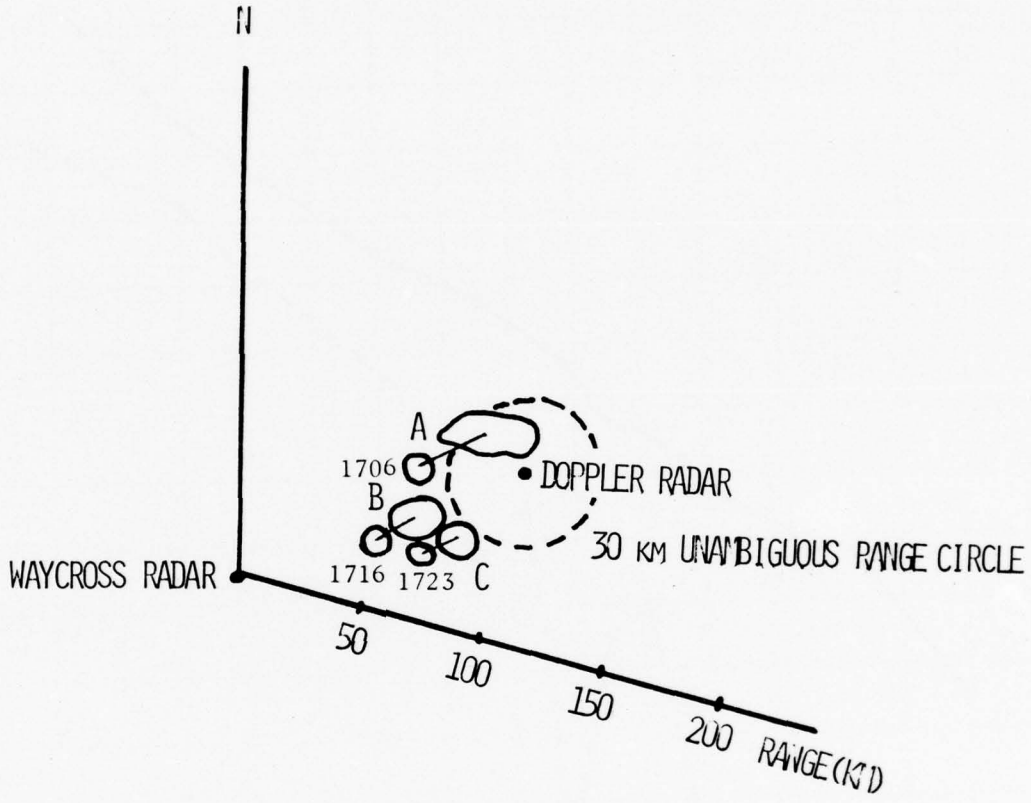

Figure 9 Location of Calspan Doppler Radar and PPI display from WSR-57 located at Waycross, Ga. for 1737 EDT, 23 June 1974 showing cell motion and location of cells observed by Doppler radar.

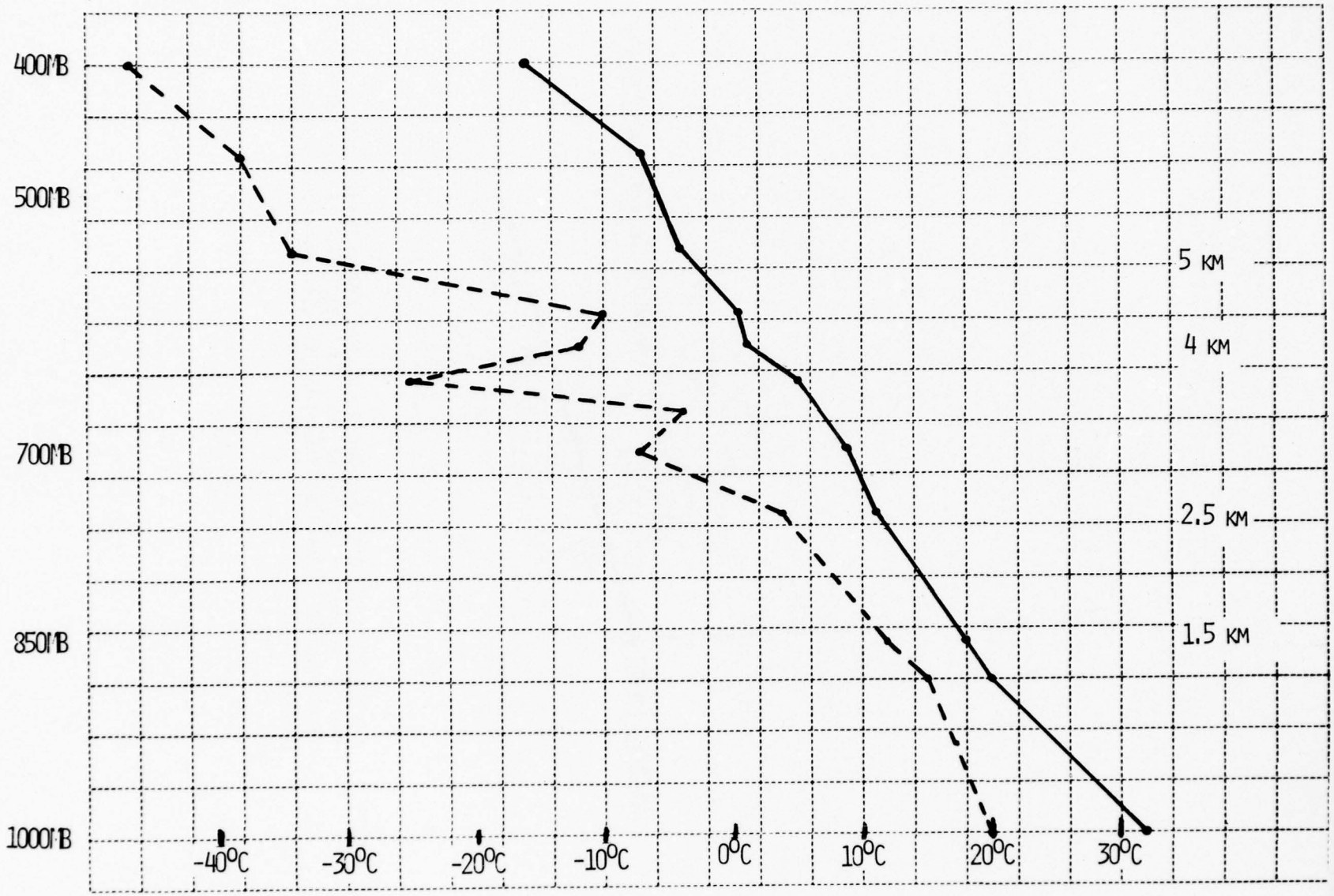

Figure 10 Temperature (solid line) and dewpoint (dashed line) sounding from radiosonde taken at Waycross, Ga., at 1400 EDT, 23 June 1974.

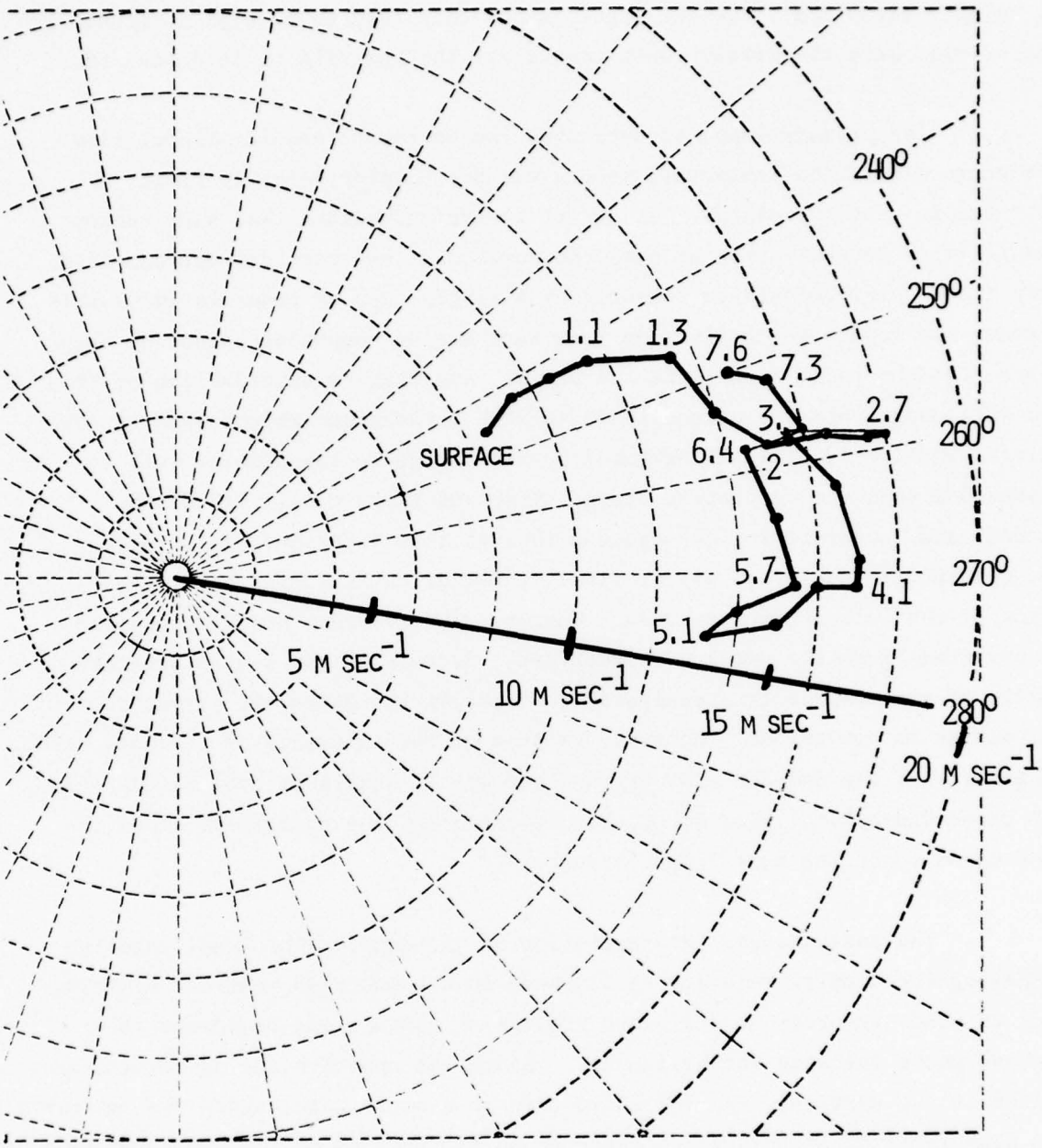

Figure 11 Hodograph of winds from radiosonde taken at Waycross, Ga. at 1400 EDT, 23 June 1974.

at heights below 3km. The RHI scans, since they reached to high altitudes in the storms, were the primary data source for the analysis to be discussed.

The primary input to determination of the three-dimensional flow structure within the convective storms was the doppler velocity field measured in vertical planes. It cannot be overemphasized that simultaneous, quantitative determination of both the horizontal and vertical motions from only the doppler velocities measured by a single doppler radar is impossible because the relative contribution from each motion component cannot be determined from the radar data alone. A useful, qualitative unscrambling of the two wind components was accomplished through a technique which compared the environmental wind field as measured by radiosonde to the doppler velocity measured within the convective storm. Time and space continuity of the updraft and downdraft regions deduced through this technique was insured. The continuity check used all available information including horizontal scans by the Calspan doppler radar, Waycross WSR-57 radar observations and observations from the surface mesonetwork. Because of the semi-quantitative nature of the unscrambling analysis, the updraft and downdraft structure arrived at is not unique. However, because of the insurance of time and space continuity of the deduced flow through use of all available data on the storm, the three-dimensional flow structure presented for the convective storm is considered to be the most likely structure.

The analysis and interpretation of the doppler RHI scans involved comparing the doppler velocity in the scan to the observed vertical distribution of winds in order to delineate regions of updraft and downdraft from regions where the wind was horizontal. Since the updrafts and downdrafts were tilted in the vertical, the RHI slice through a storm intercepted the updrafts and downdrafts at heights which depended on the azimuth of the RHI relative to the storm. In order to interpret the RHI data the previously described updraft-plane model was developed and employed.

As described in detail in Appendix A, the doppler velocity at each range and elevation angle in the RHI scan was analyzed as follows. First the

fall velocity component to doppler velocity was subtracted out using the Rogers (1964) technique. Under the assumption of no vertical motion, the angle which the environmental wind at the appropriate height would have to be rotated to produce the corrected doppler velocity, RV, was calculated. This calculation took into account all the viewing angle geometry of the observation. The computations were performed and subsequently plotted by computer. The concept of this analysis was that small rotation angles would be interpreted as horizontally moving environmental air while large rotation angles would be interpreted as updraft or downdraft.

These fields of angle of wind rotation ($\Delta\ \theta$) were analyzed as follows:

(1) In conjunction with the RV field, the rotation angle field was examined for the possible X-Z location of the updraft in the RHI scan.

(2) The possible updraft position was then used to estimate the intersection of the RHI scan and the updraft plane.

(3) The rotation angle field was then analyzed by examining the questions:

(A) If the rotation angle was large was the air in the updraft?

(B) If the rotation angle was small was the air in a location in which it could be undisturbed environmental flow?

(C) Were there any rotation angles of opposite sign to those associated with the updraft which indicated the location of the downdraft?

The final pattern of airflow was examined for time and space consistency with the Waycross radar observations, doppler PPI scans, and other RHI doppler scans. This analysis was applied to doppler data taken in four individual cells, Cells A, B, and C in Fig. 9 and Cell E which developed after 1737EDT on 23 June.

The doppler radar sampling procedure was to alternate a set of PPI scans with a set of RHI scans. The azimuth of the RHI scan was usually taken

through the portion of the storm which showed the deepest echo. As such, these RHI scans probably have a bias toward the updraft portion of the storm.

RHI Taken Along 313° at 1746EDT, 23 June

An RHI scan was obtained at 1746 EDT along an azimuth of 313° through Cell A. (See Fig. 9). The doppler velocity in (m/sec) (negative values are toward the radar) corrected for fall velocity is shown in Fig. 12. The positive center sloping upward between 3 and 5km height and at a range of 14 to 17km is the updraft. Since 313° azimuth is almost at right angles to the low-level source flow direction of 240°, the doppler velocity in the positive RV area is mostly upward motion. The absence of detectable precipitation below 2km at the 14km range (A) is consistent with the cloud base height of 1.5km derived from the Waycross sounding (Fig. 10). The rest of the RV field is interpreted using the analysis scheme outlined above which computed the rotation angle for the environmental wind.

The $\Delta\ \theta$ field is shown in Fig. 13. The updraft region appears as the large area of negative rotation (A)(negative is counterclockwise rotation to smaller wind directions) showing that with the assumption that the positive RV is horizontal wind the direction must be rotated around to the vicinity of 220°.

At mid level altitudes, regions of small rotation ($\pm$ 10°) are found at the 3 to 4km height between the 8 to 13km range. (In the following discussions, height locations will be given first followed by range location.) These regions of small rotation are interpreted as areas of no vertical motion in which environmental air, which has received its precipitation from the updraft above it, is moving horizontally. The following analysis shows that the precipitation in this air did not come from the main Cell A, but from a secondary Cell A' located near the 12km range.

The presence of Cell A' was more evident in an RHI scan taken along 313° just prior to the one shown in Fig. 12. The RV and $\Delta\ \theta$ fields for this RHI are shown in Fig. 14 and 15. The updraft for Cell A' is seen as the near

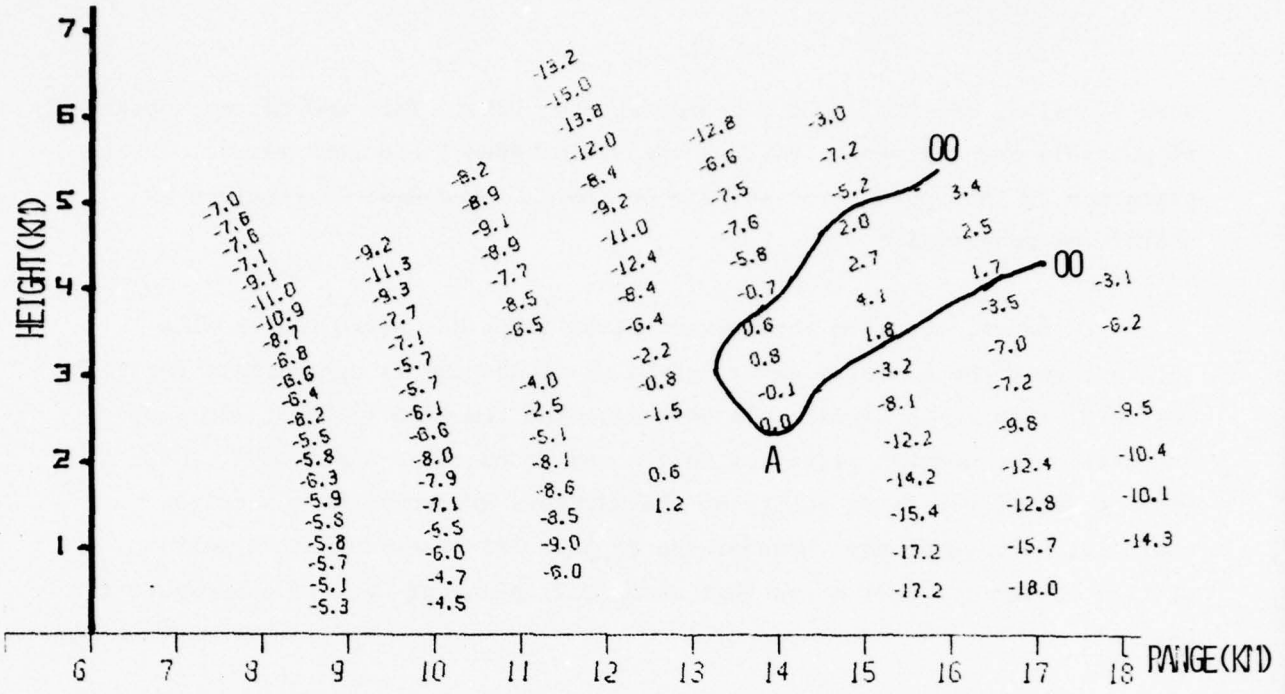

Figure 12 Field of Doppler velocity corrected for particle fall velocity (RV) for Azimuth 313°, 1747 EDT, 23 June 1974.

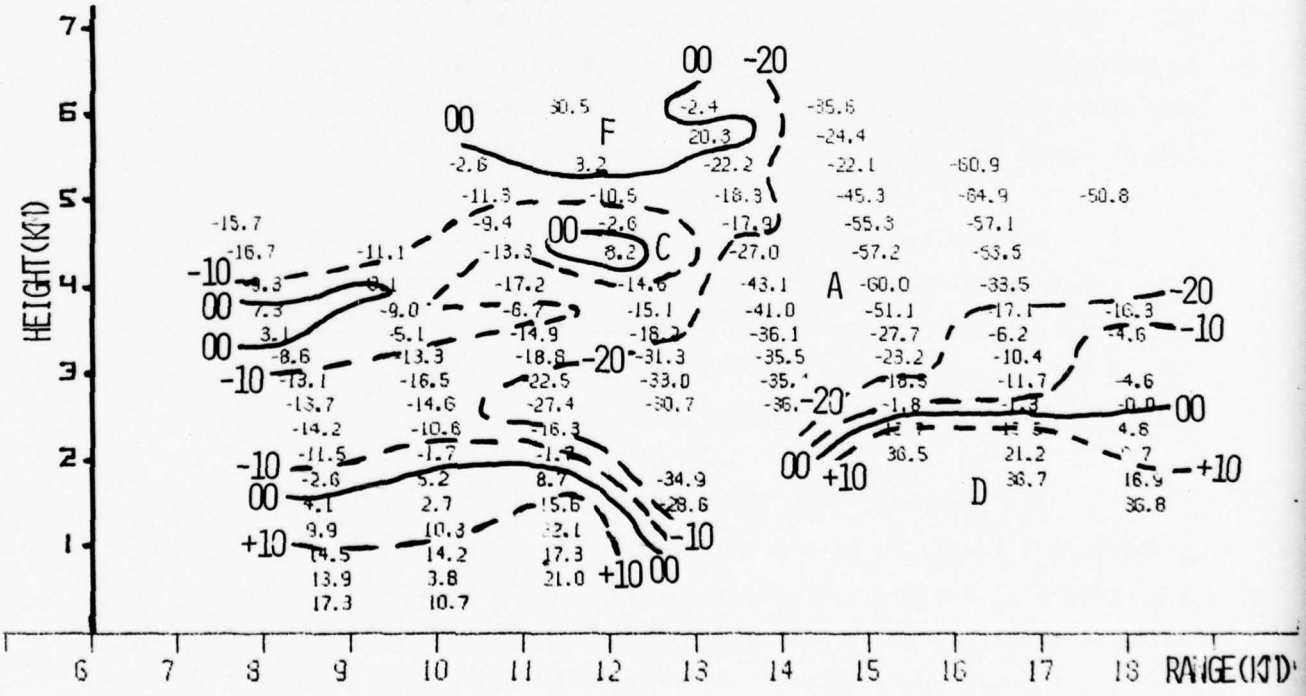

Figure 13 $\Delta\theta$ Field (see text) for Azimuth 313°, 1747 EDT, 23 June 1974.

zero RV values and the -30 $\Delta\theta$ center at 3km, 12km. This updraft was apparently responsible for the precipitation observed between 8 and 13km range. Interpretation of the upper levels of the $\Delta\theta$ field around Cell A' required an updraft-plane analysis.

Experience with the updraft-plane model has shown that a wind located above the boundary layer and below cloud base is appropriate for the low level wind in the model. In this case the 1km wind (243° at 12m/sec) was used. The updraft plane for Cell A was found to be along 280°. Cell A' was not detectable as an entity on the Waycross PPI scans so its motion could not be determined. However the doppler PPI scans suggest a motion similar to that of Cell A, so that an updraft plane of 280° is reasonable for Cell A'.

Fig.16 is a schematic showing the azimuth of the RHI, the updraft plane through Cell A' at 3km, and the +8 $\Delta\theta$ center at 4km, 12.5km in Fig.13, (C) . Both the 4km air and the updraft plane were displaced backward in time to positions indicated by (1). With a reasonable location for the updraft at 4km along the updraft plane at time (1), this analysis indicates that the +8$\Delta\theta$ center could have received its precipitation from updraft A'.

Another area in the $\Delta\theta$ field which suggested precipitation falling into horizontally moving air is the region with values between +10 and -10 which was located underneath the major updraft beyond 15km range (D) in Figs. 13 and 15. A similar structure is seen in the region (E) of the secondary Cell A' between 8-11km range (Fig. 15).

The downdraft from the secondary Cell A' is indicated in the positive $\Delta\theta$ field (F) at 6km height and 12km range in both Figs.13 and 15. A downdraft is strongly suggested by the missing data point in the $\Delta\theta$ field in each of these areas. The corresponding RV fields show continuously large negative through this region. The program for computing $\Delta\theta$ has a provision which does not compute $\Delta\theta$ when the cosine of the rotation angle is greater than $\pm$ 1. This condition exists when RV is greater than the component of the

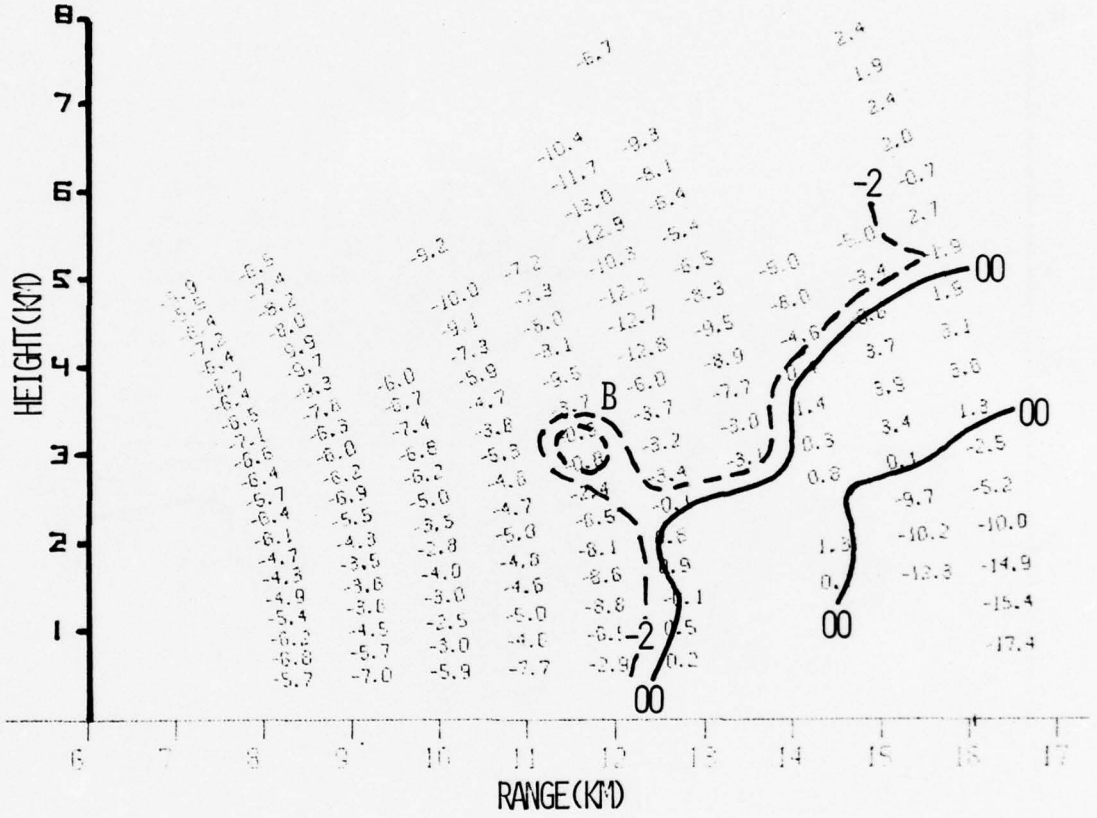

Figure 14 RV field (cf. Fig. 12) for Azimuth 313°, 1745 EDT, 23 June 1974.

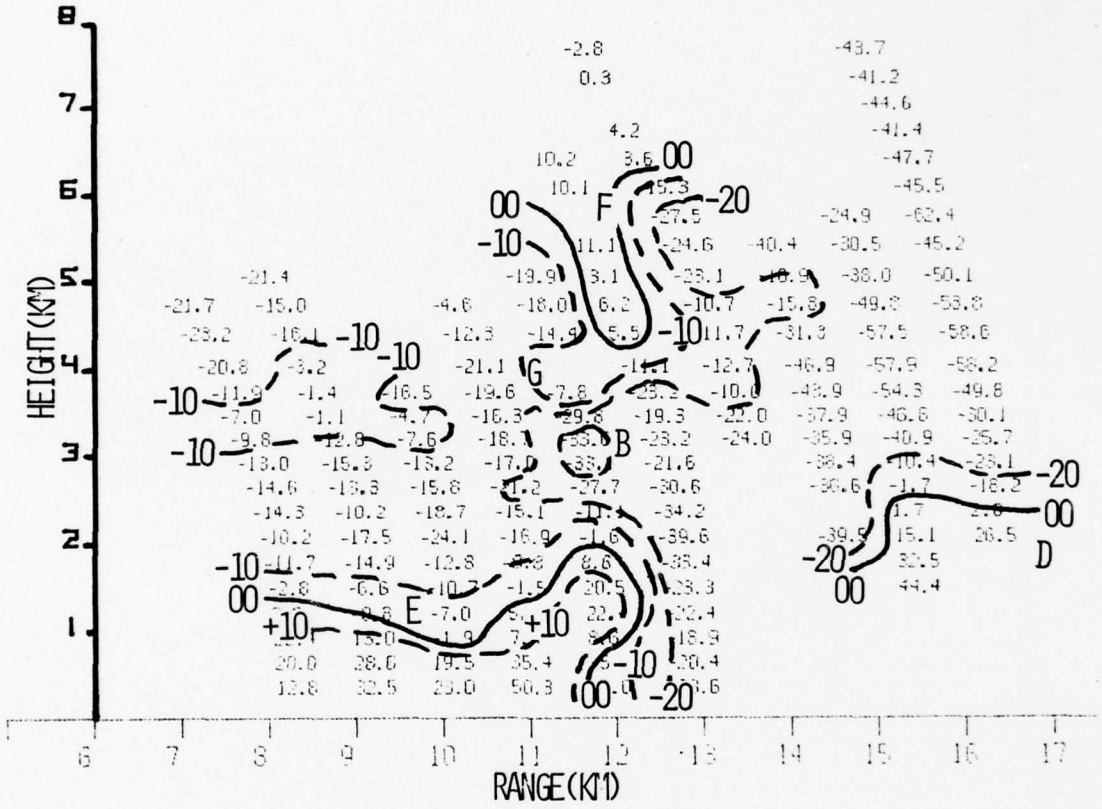

Figure 15 $\Delta\Theta$ field for Azimuth 313°, 1745 EDT, 23 June 1974.

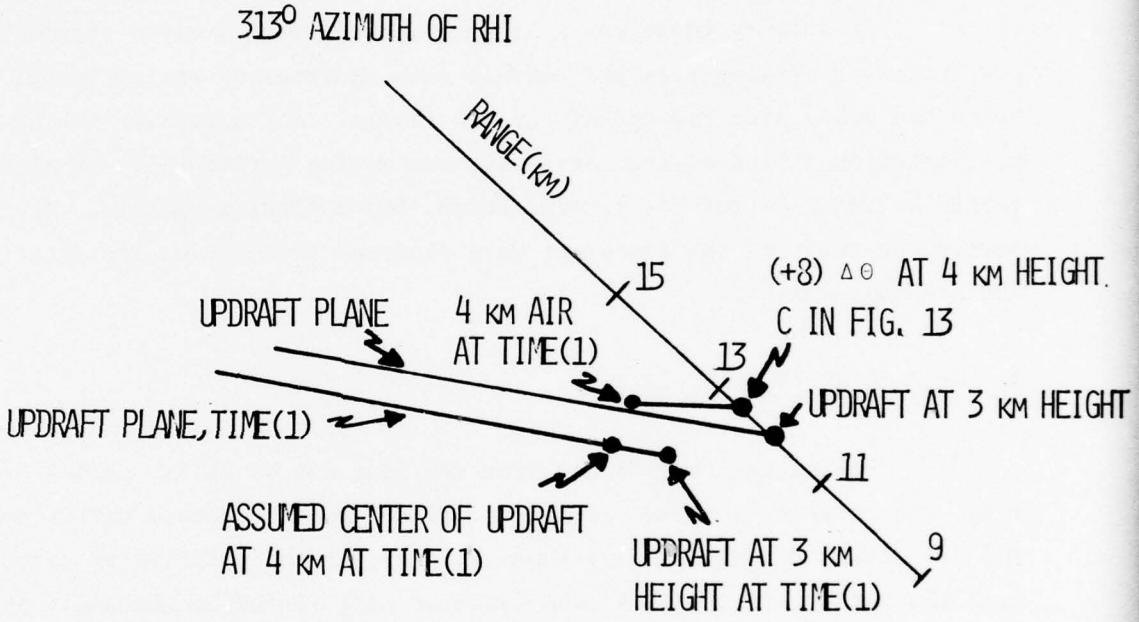

Figure 16 Possible history of downdraft air found at 4km height in Azimuth 313°, 1747 EDT, 23 June 1974.

observed wind along the radar beam (Reference Appendix A). In the present case where large negative RV values exist at large elevation angles, part of the RV must be a result of downward motion. If this downward motion is assumed to be horizontal motion, the resulting RV value cannot be accounted for by rotation of the observed environmental wind. Both downward motion areas are located in a position to be related to Cell A' with the updraft at 3km, 12km. There is another missing $\Delta\ \theta$ at 4km, 11.5km (G) Fig. 15 which indicates a downdraft at this level possibly for Cell A.

In summary there was a sloping updraft from a major storm with precipitation falling from the updraft into undisturbed environmental flow below and along side the updraft at low levels. For a smaller secondary cell, precipitation filled environmental air was moving horizontally at middle levels having received its precipitation from a sloping updraft. At middle levels the roots of the downdraft were observed to receive precipitation from the sloping updraft.

RHI at 340° at 1758EDT, 23 June.

During the ten minutes from the last set of RHI's, Cell A became large and complex, and the secondary Cell A' grew and became better organized. The RV pattern for this RHI is shown in Fig. 17; the positive RV associated with the updraft from Cell A' was found at (A') (3-4km height and 4 to 8km range) and the updraft for Cell A was located between 10 and 17km at the same height interval (A). The positive RV values were a little larger since at this azimuth a 240° wind had a small positive component along the RHI scan azimuth. The updrafts are seen to slope upward away from the radar.

In Fig. 18 the updrafts show up as large regions of large negative $\Delta\ \theta$. The region of horizontally moving environmental air (-10 to +10) is seen beneath each of these updrafts. Notice how the region broadens in the vertical underneath the higher portion of the updrafts, particularly with Cell A at (B) (range 14 to 16km). This region is where the downdraft with roots around 4km would not be expected primarily because the 270° wind direction brings the 4km

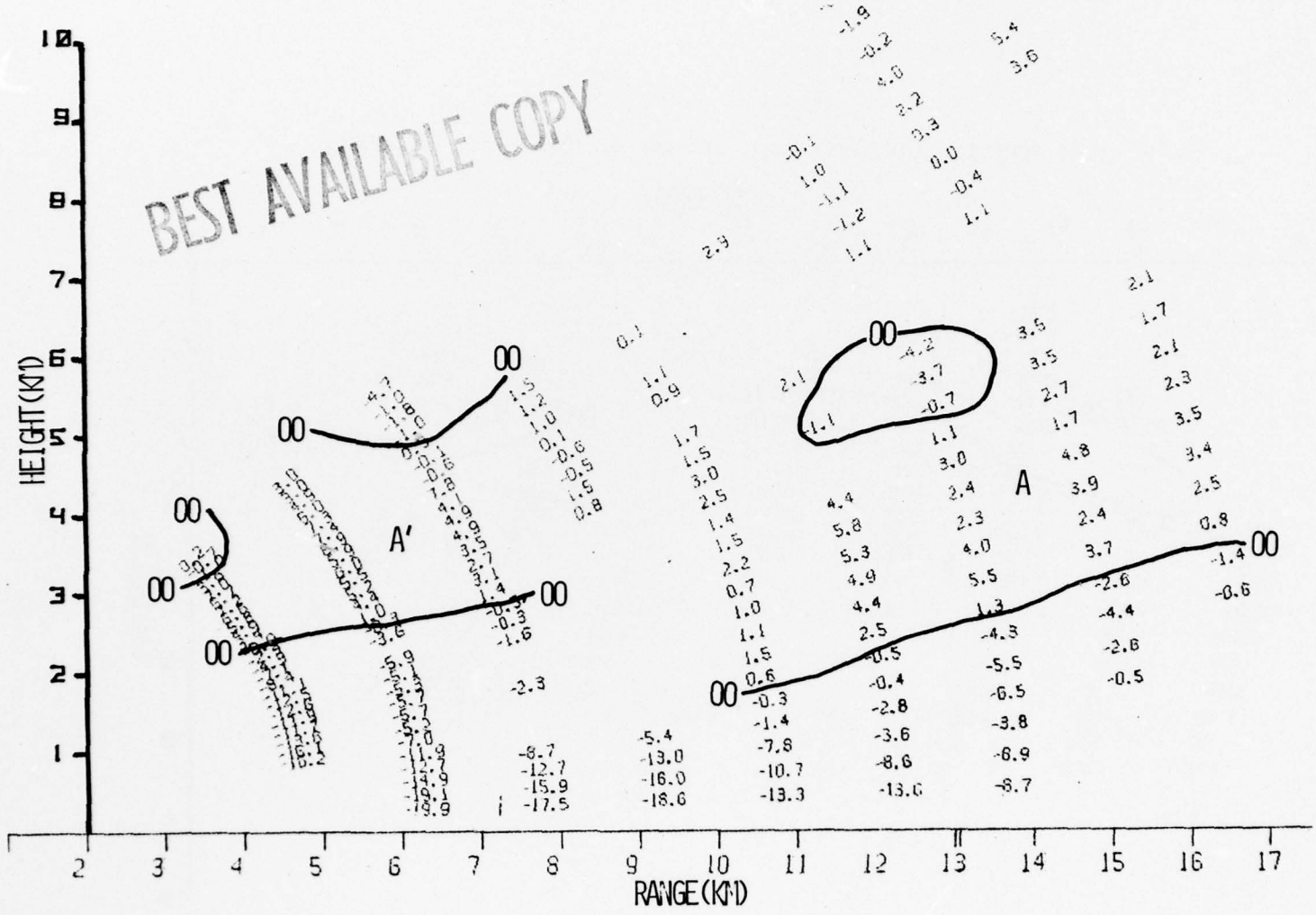

Figure 17 RV field (cf. Fig. 12) for Azimuth 339°, 1758 EDT, 23 June 1974.

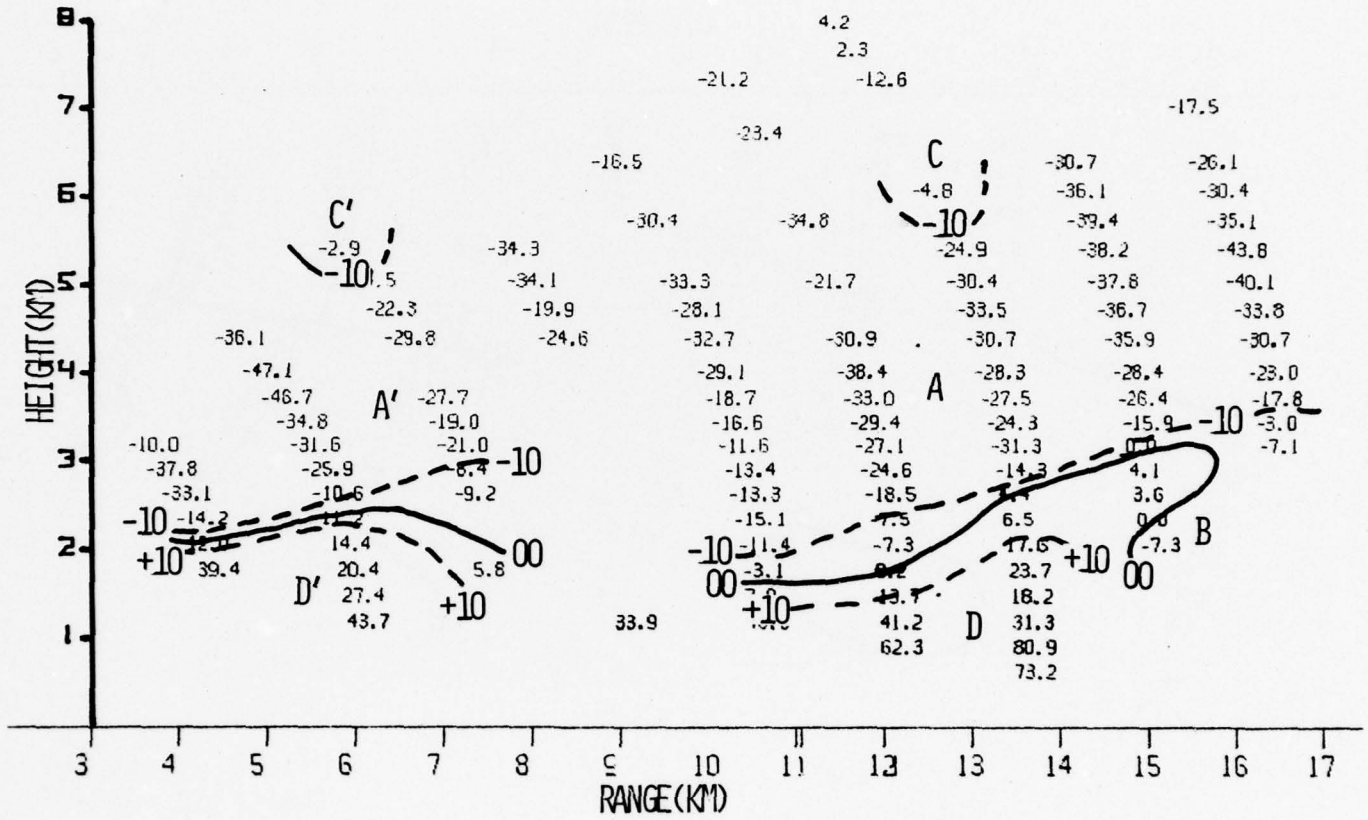

Figure 18 $\Delta\Theta$ field for Azimuth 339°, 1758 EDT, 23 June 1974.

air closer to the radar. Thus underneath the updraft, precipitation filled environmental air exists through a 1km deep layer and shows up as the broad region of $\pm$ 10 $\Delta\Theta$.

Only a couple of spots of horizontally moving air (with precipitation) are seen at 6km height at 6 and 13km ranges (C') and (C). The small amount of horizontally moving air is attributed to the RHI slice having been taken near the center of the updraft. With a 280° updraft plane the RHI is located at 60° to this plane. The indication of the downdraft by the rotated wind direction value around 270° in the positive $\Delta\ \theta$ area was found underneath the updrafts (D') and (D).

Another RHI was taken 10° further west, and the $\Delta\ \theta$ field is shown in Fig. 19. This RHI slice cut through the northern edge of the updraft for Cell A' at 4km between 11-12km range and the southern edge of the updraft for Cell A at 5km and 14-15km. In the computed wind field, the 270°-280° directions are found in a shallow layer under the updrafts and run along just underneath the zero $\Delta\ \theta$ region at the 2km height (B) and (B'). The downdraft at upper levels is indicated between 6 and 7km at 12km range by the large positive $\Delta\ \theta$ (C). The updraft plane analysis indicates that this 6.5km air could have received precipitation from an updraft at or above 7km before arriving at this azimuth.

At 1800EDT attention was switched from Cell A to the north to Cells B and C as they approached within radar range to the west and southwest. First, however, Cell E developed to the west of the radar and was sampled by an RHI at 1808EDT.

RHI at 278° at 1808EDT, 23 June, Cell E

In this RHI the radar is looking into Cell E approaching the radar from upwind rather than into the side of a cell moving by the radar, as in the previous RHI's. The Waycross radar data indicate that this RHI was taken through at least two cells. Cell E to the west-northwest of the radar and

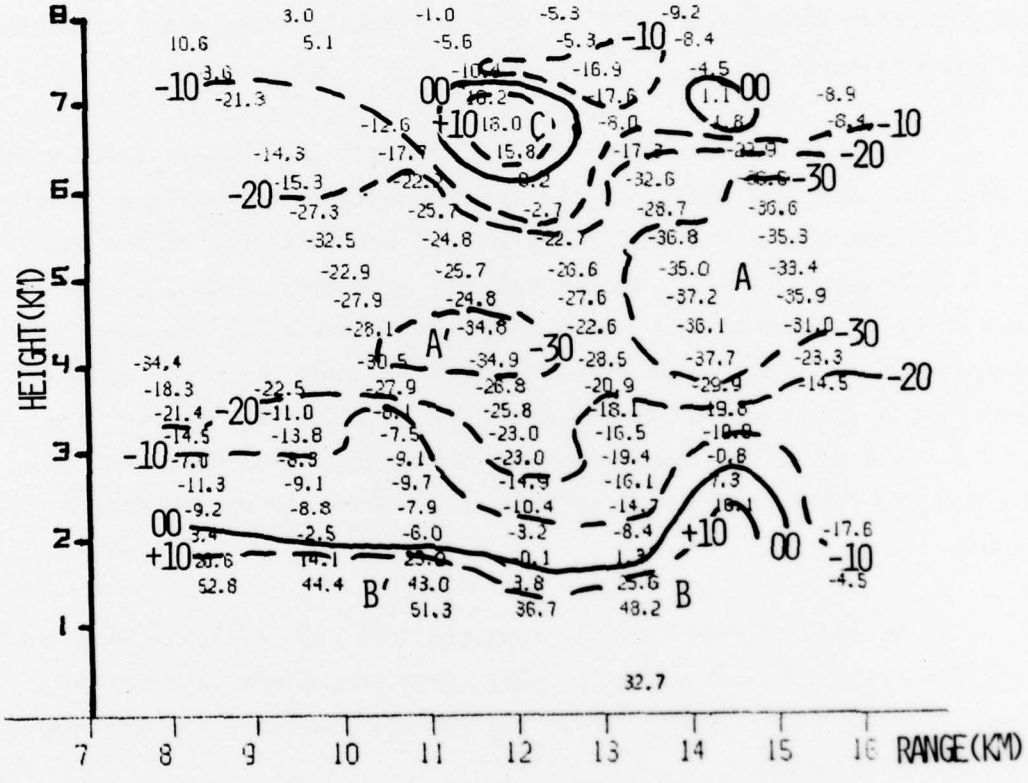

Figure 19 $\Delta\theta$ field for Azimuth 330°, 1756 EDT, 23 June 1974.

Cell B to the west. In the RV field in Fig. 20 the near zero,negative region (A) at 3km, 5.5km is the updraft from Cell E while positive RV (B) above 4km and around 9km range is from Cell B.

In Fig. 21 the large, negative $\Delta\theta$ (C) at 3km, 5km shows the updraft from Cell E. The absence of precipitation above this region suggests the doppler radar was looking at the southern edge of the 280° updraft plane so that no updraft was found above the 3km level. The Cell B updraft is characterized by the very large, negative rotation angles (D).

The downdraft from Cell B is the least negative region of $\Delta\theta$ (E) at 3-4km and 7-8km range. The RV field is continuous in this region so that the missing data point (E) in the $\Delta\theta$ field indicates downdraft. In this RHI the radar was looking at the region underneath the updraft at high levels (a region which was not sampled in the previous RHI scans) and therefore sampled the downdraft.

Sequence of vertically pointing data 1811-1814EDT. 23 June

Between 1811 and 1813:30 EDT the doppler antenna was pointed vertically and observations were taken at 1 sec intervals. The doppler velocities were corrected for fall velocity and every fifth observation was plotted. These data are shown in Fig. 22. For a cell moving with a 16m/sec. speed, the 2.5 minute observation interval converts to 2.5km in space.

In detail the vertical velocity field is complex, a not unexpected result in view of the various origins of the air which arrive in a vertical column at any instant of time. This complexity is compounded by the presence of at least three cells: B, C and E in the area of the radar during this time. Therefore, only broad interpretations of the vertical velocities in terms of the individual cells was attempted.

In the broad sense, this sequence fits the sloping updraft model. The downdraft (A) located between 4 and 5km (Figure 22), which sloped upward

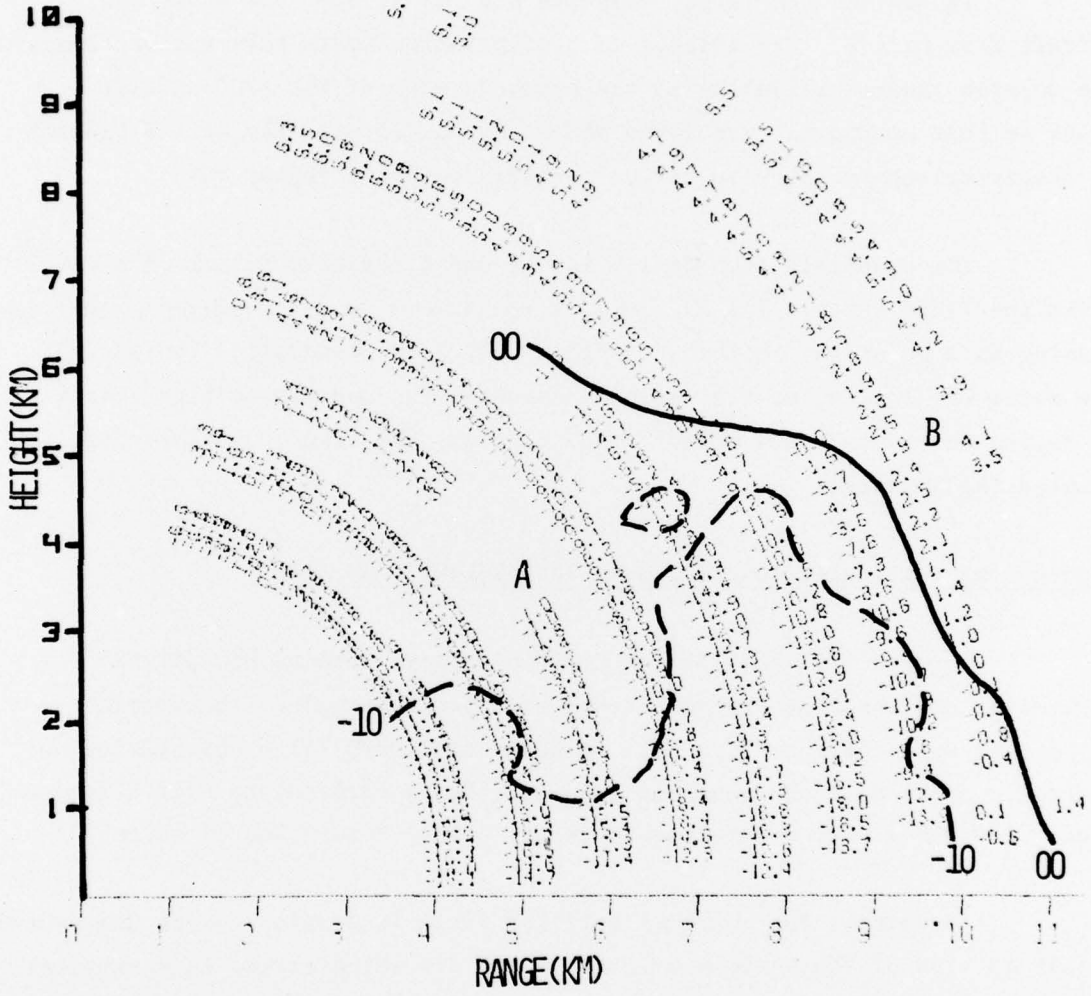

Figure 20 RV field (cf. Fig. 12) for Azimuth 278°, 1808 EDT, 23 June 1974.

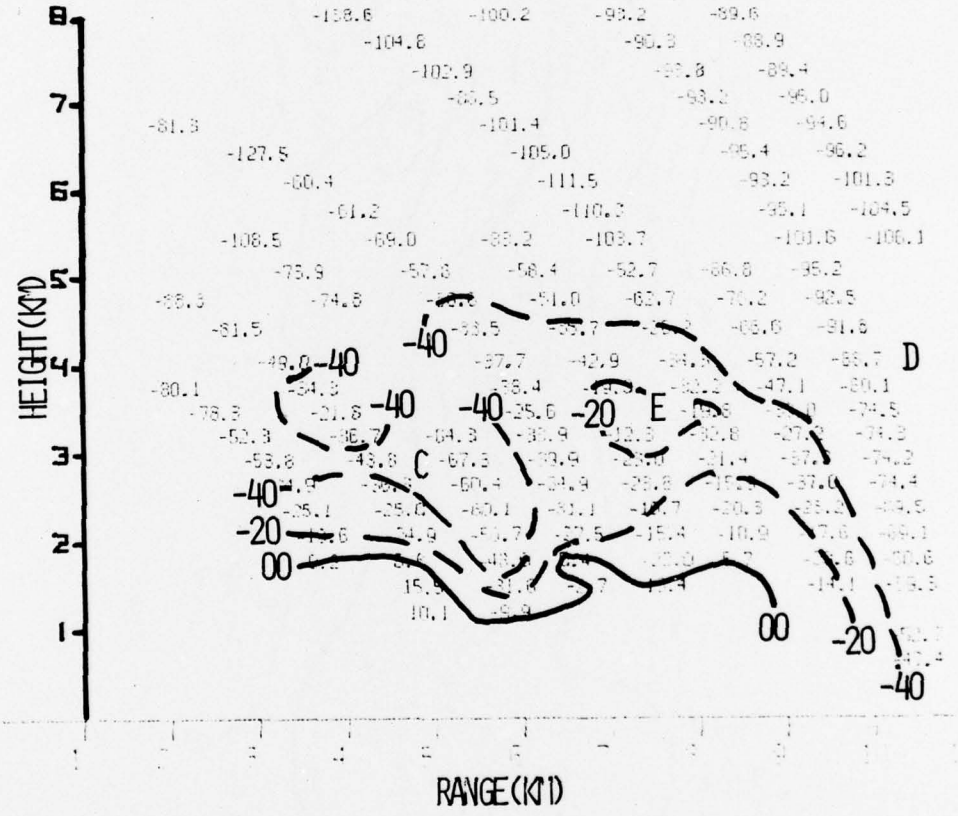

Figure 21 $\Delta\Theta$ field for Azimuth 278°, 1808 EDT, 23 June 1974.

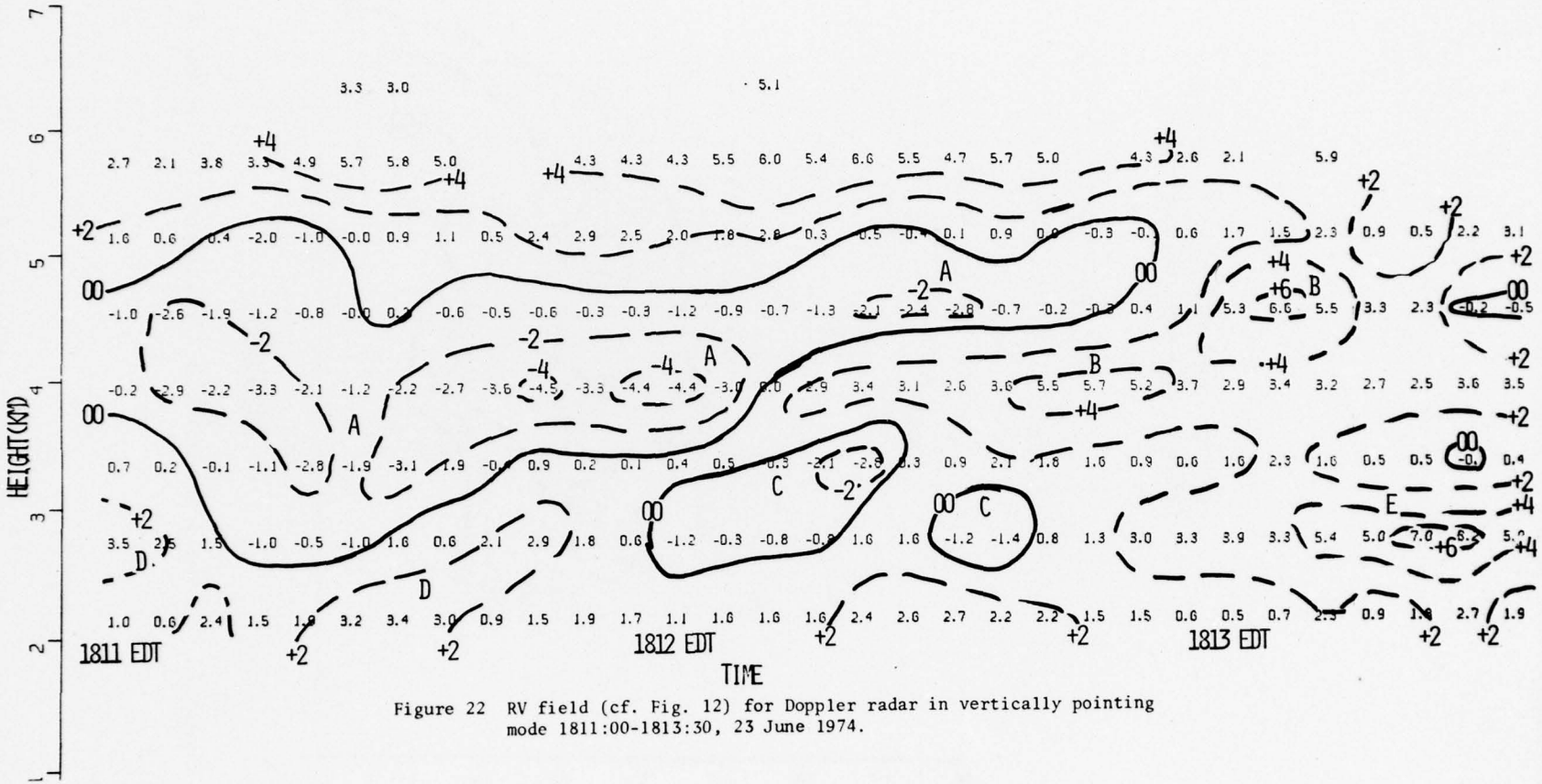

Figure 22 RV field (cf. Fig. 12) for Doppler radar in vertically pointing mode 1811:00-1813:30, 23 June 1974.

with time, is consistent with a storm approaching from the west, in this case probably Cell C. The stronger downward velocity values (-4m/sec.) at 4km fit with the dry layer located at 4 km. The updraft (B) between 4 and 5km slopes upward as would be expected as a cell approached, probably Cell B. The downdrafts (C) located underneath this updraft at earlier times were probably generated by this updraft. The updraft (D) at 2-3km at the beginning of the sequence is the lower portion of the updraft from Cell E. The updraft (E) at 2-3km height observed late in the sequence cannot be explained in a manner consistent with the interpretations given for the other updrafts and downdrafts.

RHI at 208° at 1824 EDT, 23 June, Cells C and B

In this RHI the viewing angle relative to storm motion is different from previous viewing angles. In this case the radar was looking into the environmental winds and into the storm from the north as it moved eastward. Figure 23 shows the RV field for this RHI. From Waycross radar data the region out to 8km was Cell B; the region beyond 8km was Cell C. Cell C moved slightly differently than Cell A and therefore produced an updraft plane along 303°. This RHI was then almost at right angles to the updraft plane, so that the slice is across the updraft rather than along it.

Notice in Figure 23 that the RV field below 8km is all negative because of the azimuth and the environmental wind directions of 240°-280°. Updrafts are difficult to locate in this RV field since they tend to be minima produced by upward moving air with 240° winds. However, minima could also occur with environmental wind of 270° ($\sim$ 60° to the azimuth of the RHI). This ambiguity points up the need for processing the doppler velocity data by some objective scheme.

Figure 24 presents the $\Delta\theta$ field for this RHI. At this azimuth, interpretation of the sign of $\Delta\theta$ in terms of updraft and downdraft is reversed from that which held for the other azimuths. For example, the small negative

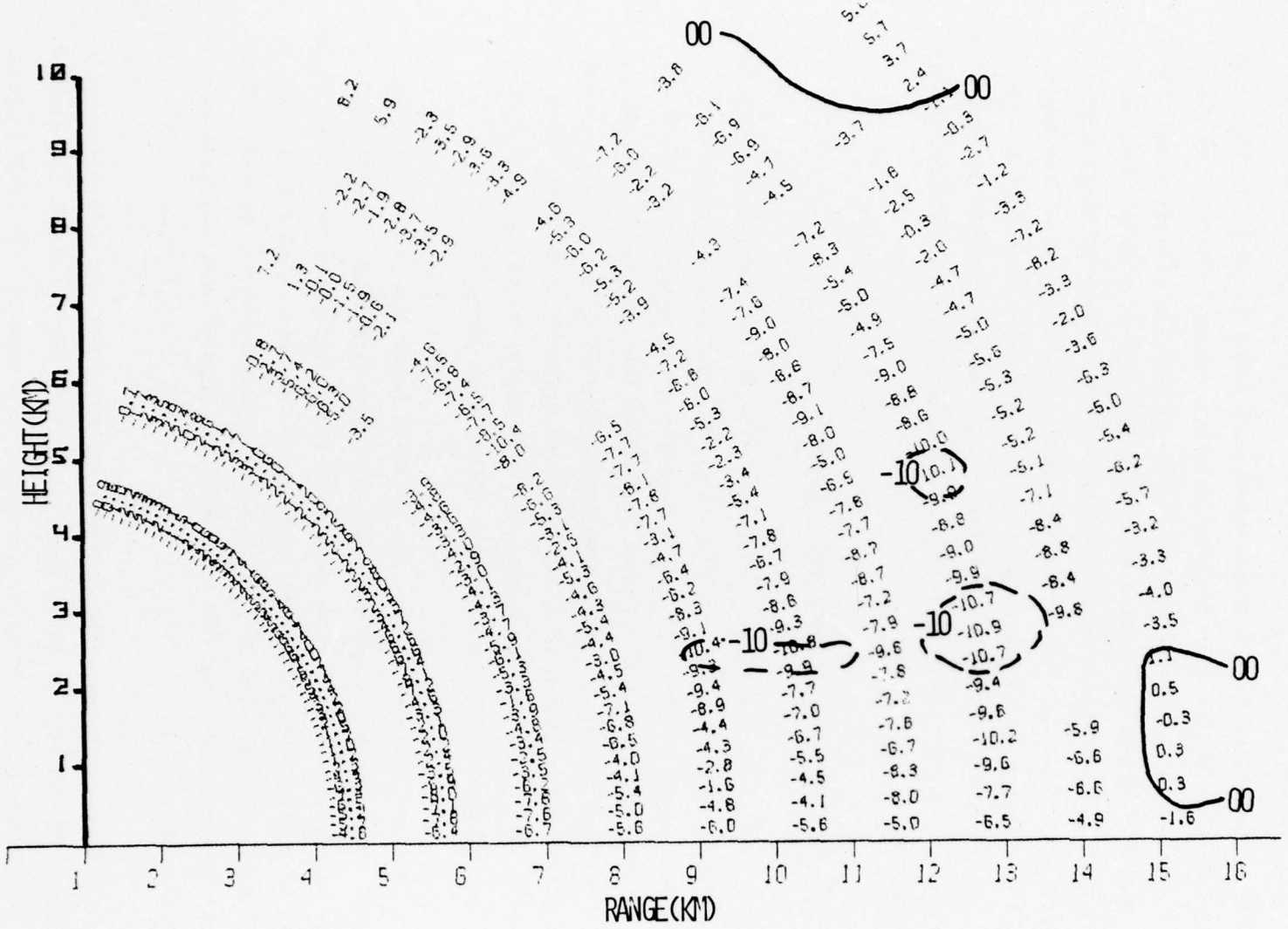

Figure 23 RV field (cf. Fig. 12) for Azimuth 208°, 1824 EDT, 23 June 1974.

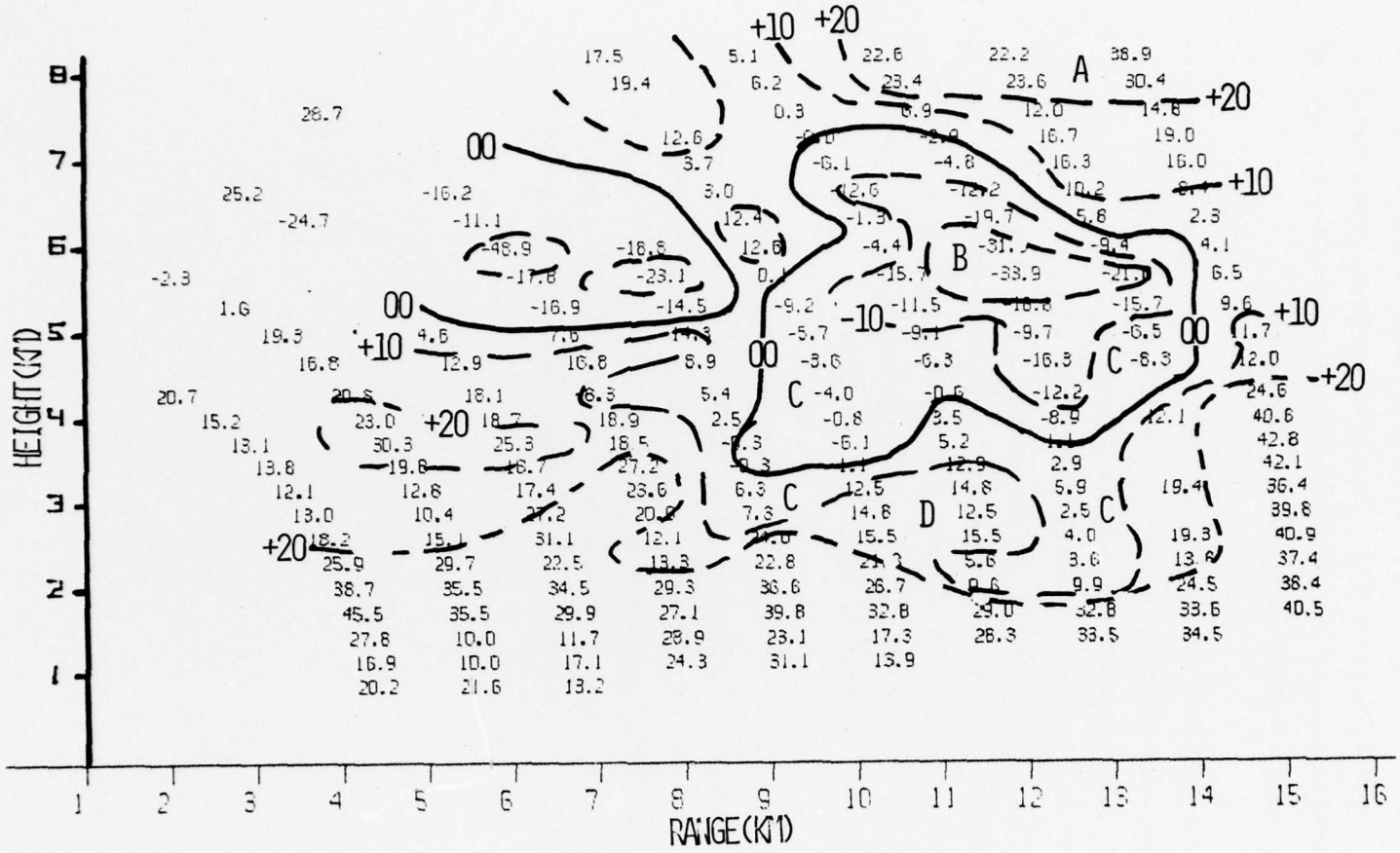

Figure 24 $\Delta\Theta$ field for Azimuth 208°, 1824 EDT, 23 June 1974.

values in the RV field in the updraft are accounted for by rotating the wind clockwise to larger angles (positive $\Delta\theta$). On the other hand, large negative RV values from downdrafts must be accounted for by rotating the wind counterclockwise to provide more component along the RHI azimuth.

The Waycross PPI data show that this RHI cut through the rear portion of Cell C. Thus, the positive $\Delta\theta$ region (A) (Figure 24) between 6.5 and 8km height and 10 to 14km range is the updraft from Cell C. The slope upward of the updraft toward the radar is consistent with the slope of the updraft plane along 303°. The negative area (B) between 5-6km and 11-13km range is the downdraft. This analysis is consistent with backward trajectories of the air at 5.5km and the backward displacement of the updraft plane to 1822EDT. The 1822EDT position of the updraft plane was consistent with the updraft location at 1.5km height on the doppler PPI taken at 1822.

The regions of -10 to +10 $\Delta\theta$ (C) between 9 to 13km and below 4km are regions of undisturbed environmental flow receiving their precipitation from aloft. The bulge of +10 to +15 $\Delta\theta$ (D) between 2 to 3km altitude and 10 to 12km range is in a position where it could be the low level portion of the downdraft from Cell B. This interpretation is consistent with a 275° to 280° wind at 1km observed in the doppler PPI scans taken earlier at 1822EDT.

REFERENCES

1. Brown, R.A. and K.C. Crawford, 1972: Doppler Radar Evidence of Severe Storm High-Reflectivity Cores Acting as Obstacles to Air Flow, Proceedings 15th Radar Meteorology Conference, Boston, Amer. Meteor. Soc.

2. Easterbrook, C.C., 1974: Continued Studies of Coastal Convective Storms Utilizing Doppler Radar. Technical Report No. CK-5077-M-3, Calspan Corp., Dec. 1974.

3. Easterbrook, C.C. 1975: Estimating Horizontal Wind Fields by Two-Dimensional Curve Fitting of Single Doppler Radar Measurements. Preprints, 16th Radar Meteorology Conference, Houston, Texas, Amer. Meteor. Soc., 214-219.

4. Easterbrook, C.C. and C.W. Rogers, 1973: An Area Curve Fitting Method for Analysis of Doppler Weather Radar Data with Applications to the Study of Convective Storms. Calspan Corporation Tech. Report No. CK-5077-M-1.

5. Easterbrook, C.C. and C.W. Rogers, 1974: Case Studies of Coastal Convective Storms as Observed by Doppler Radar. Technical Report No. CK-5077-M-2, Calspan Corporation, April 1974.

6. Fankhauser, J.C., 1971: Thunderstorm-Environment Interactions Determined from Aircraft and Radar Observations, Monthly Weather Review, 99, p. 171-192.

7. Kropfli, R.A. and L.J. Miller, 1975: Kinematic Structure and Flux Quantities in a Convective Storm from Dual-Doppler Radar Observations, J. Atmos. Sci., 33, 520-529.

8. Rogers, R.R., 1964: An Extension of the Z-R Relation for Doppler Radar. Proc. Eleventh Radar Weather Conf., Boston Amer. Meteor. Soc., 158-161.

Appendix A

Analysis of Doppler Velocity in RHI Scan to Produce Rotation Angle ($\Delta\Theta$) of Observed Wind

The equation for doppler velocity is

$$V_d = V_H \cos \Theta \cos \phi + W \sin \phi + WF \sin \phi \qquad (1)$$

where V_d = measured doppler velocity, negative toward the radar

V_H = horizontal wind speed

Θ = angle between wind direction and azimuth of radar RHI

$\Theta = 0^\circ$ is a wind along RHI azimuth in the direction of increasing range; Θ increases clockwise

ϕ = elevation angle of radar beam

W = vertical velocity, negative downward

WF = fall velocity of precipitation, negative downward

Since the purpose of the analysis of the doppler velocity field is to qualitatively specify V_H and W, V_d is first corrected for fall velocity. WF is computed from the signal intensity using Rogers' technique (1964). The vertical velocity component to V_d is removed from V_d to produce a doppler velocity corrected for fall velocity, defined as RV.

$$RV = V_d - WF \sin \phi = V_H \cos \Theta \cos \phi + W \sin \phi \qquad (2)$$

RV is analyzed in the following manner:

(1) Assume that the vertical motion is equal to 0. Then assume that at a given height the wind speed of the rawinsonde observed environmental wind is correct. Then ask what direction would this wind speed have to be in order to produce the observed RV. That is

$$\Theta = \arccos \frac{RV}{V_H \cos\phi} \qquad (3)$$

(2) From the new wind direction, the angle $\Delta\Theta$, that the environmental wind must be rotated to produce RV is computed. The sign convention is:

$\Delta\Theta$ = negative, the wind direction is reduced

$\Delta\Theta$ = positive, the wind direction is increased